



Biased MJO causing a lack of QBO–MJO connection in multi-model simulations with a nudged QBO

Kai Huang¹, Chang-Hyun Park², Seung-Yoon Back^{2,3}, Jorge L. García-Franco⁴, Hera Kim^{2,5}, Pu Lin^{6,7}, Scott Osprey^{8,9}, Jadwiga Richter¹, Chih-Chieh Chen¹, Seok-Woo Son², Shigeo Yoden¹⁰, Yuna Lim^{11,12}, Neal Butchart¹³, James Anstey¹⁴, Yoshio Kawatani¹⁵, Martin B. Andrews¹³, Francois Lott¹⁶, Yixiong Lu¹⁷, Zhaoyang Chai¹⁸, Nan Rosenbloom¹, Qi Tang¹⁹, Jinbo Xie^{19,20}, Federico Serva²¹, Dong-Chan Hong², Shingo Watanabe^{22,23}, Aleena M. Jaison²⁴, Hiroaki Naoe²⁵, and Kohei Yoshida²⁵

¹National Science Foundation National Center for Atmospheric Research, Boulder CO, 80305, USA

²School of Earth and Environmental Sciences, Seoul National University, Seoul, 08826, Korea

³The Department of the Geophysical Sciences, The University of Chicago, Chicago IL, 60637, USA

⁴National School of Earth Sciences (Escuela Nacional de Ciencias de la Tierra), UNAM, Mexico City, 04510, Mexico

⁵Department of Atmospheric Sciences, University of Washington, Seattle, WA, USA

⁶Department of Earth and Environment Science, Boston College, Chestnut Hill, MA, USA

⁷Geophysical Fluid Dynamics Laboratory(NOAA), Princeton, NJ, USA

⁸Department of Physics, University of Oxford, Oxford, UK

⁹National Centre for Atmospheric Science, Oxford, UK

¹⁰Professor Emeritus of Kyoto University, Kyoto, 606-8501, Japan

¹¹Earth System Science Interdisciplinary Center, University of Maryland College Park, College Park, MD, 20740, USA

¹²Global Modeling and Assimilation Office, NASA Goddard Space Flight Center, Greenbelt, MD, 20771, USA

¹³Met Office Hadley Centre (MOHC), Exeter, UK

¹⁴Canadian Centre for Climate Modelling and Analysis, Environment and Climate Change Canada, Victoria, British Columbia, Canada

¹⁵Faculty of Environmental Earth Science, Hokkaido University, Sapporo, Japan

¹⁶Laboratoire de Météorologie Dynamique (LMD), Paris, France

¹⁷State Key Laboratory of Severe Weather Meteorological Science and Technology, Earth System Modeling and Prediction Centre, China Meteorological Administration, Beijing, China

¹⁸Earth System Numerical Simulation Science Center, Institute of Atmospheric Physics, Chinese Academy of Sciences, Beijing 100029, China

¹⁹Lawrence Livermore National Laboratory, Livermore, CA, USA

²⁰High Meadows Environmental Institute (HMEI), Princeton University, Princeton, NJ, USA

²¹Institute of Marine Sciences, National Research Council (CNR-ISMAR), Rome, Italy

²²Japan Agency for Marine-Earth Science and Technology (JAMSTEC), Yokohama, Japan

²³Advanced Institute for Marine Ecosystem Change (WPI-AIMEC, Tohoku University, Sendai, Japan)

²⁴Atmospheric, Oceanic and Planetary Physics, University of Oxford, Oxford, United Kingdom

²⁵Meteorological Research Institute, Japan Meteorological Agency, Tsukuba, Japan

Correspondence: Chang-Hyun Park (sweetweather@snu.ac.kr)

Abstract. Observations suggest that the stratospheric Quasi-biennial Oscillation (QBO) modulates the Madden-Julian Oscillation (MJO) in the tropical troposphere, where the MJO is stronger with a smoother eastward propagation in the boreal winter seasons with a QBO easterly (QBOE) than that with a QBO westerly (QBOW) phase. Such connection is not captured by



5 current climate models through their internally generated QBO and MJO. The QBO initiative (QBOi) phase 2 project included
climate models from global modeling centers and conducted simulations with the tropical zonal-mean zonal wind in the model
stratosphere nudged towards the observations. This paper investigates the potential connection between the nudged QBO and
the internally generated MJO in 12 participating climate models. Results show that the stratospheric QBO and its associated
impacts on the upper troposphere and lower stratosphere stability around the equator are realistically represented in all models
10 through the nudging although a smaller amplitude is found for the temperature responses. However, there is no significant con-
nection between the QBO and MJO in any of the participating models. Further diagnostics suggest this likely result from the
biases in the internally generated MJO by the models where the simulated MJO convective variation is constantly underesti-
mated so that the intense MJO OLR and precipitation anomalies are inadequately induced. However, the QBOi phase 2 models
show no systematic bias in the MJO cloud-radiative feedback strength, with individual models spanning the full range from
15 underestimation to overestimation of the observed values. These findings emphasize the importance of accurate representation
of the MJO convective system in capturing the QBO-MJO connection by climate models. This paper also underscores the
urgency of new theoretical understandings for the observed QBO-MJO connection.

1 Introduction

The Madden-Julian Oscillation (MJO, Madden and Julian, 1971, 1972) refers to a planetary-scale organized convective system
20 coupled with a baroclinic overturning circulation in the tropics. It is characterized by an intraseasonal timescale of 20-100
days and an eastward propagating phase speed around 5 m/s (Zhang, 2005). A typical MJO case initiates and grows over the
Indian Ocean (IO), propagating eastward across the Maritime Continent (MC) and into the western Pacific (WP). Its convection
waned around the dateline, but the coupled circulation in the higher troposphere keeps propagating eastward into the western
hemisphere (Jiang et al., 2020). The MJO leaves significant impacts on the weather and climate modes in the intraseasonal
25 timescale such as its direct modulation of the tropical convective systems including the diurnal cycle precipitation (e.g., Oh
et al., 2012; Peatman et al., 2014), the mesoscale convective systems (Houze Jr., 2004; Crook et al., 2024), the tropical cyclones
(Kim and Seo, 2016), and the monsoon systems (Fu et al., 2013; Adames and Ming, 2018). It also impacts the weather patterns
in the mid-to-high latitudes through the wave-train-like teleconnection patterns (Adames and Wallace, 2014; Toride and Hakim,
2021; Tseng et al., 2020, and many others). Therefore, MJO serves as a primary source of subseasonal predictability in the
30 tropics and influences predictability beyond the tropics through teleconnections (Zhang, 2005; Jiang et al., 2020; Stan et al.,
2022).

The Quasi-Biennial Oscillation (QBO, Reed et al., 1961; EBDON and VERYARD, 1961) refers to a zonal-mean regime of
the zonal wind shear in the tropical stratosphere, alternating between easterly and westerly phases. The QBO wind shear transi-
tion usually takes about 28 months and the wind shear propagates from the higher to mid-lower stratosphere with time. Despite
35 occurring in the tropical stratosphere, but QBO is able to modulate global surface conditions (Baldwin et al., 2001; Anstey
and Shepherd, 2014; Park et al., 2022), the storm tracks (Wang et al., 2018a, b), atmospheric rivers (Huang et al., 2025b), and
tropical convection (Collimore et al., 2003; Lane, 2021). Specifically, the interannual activity of MJO is significantly modulated



by the QBO phase (Yoo and Son, 2016; Son et al., 2017), recognized as the QBO-MJO connection. It is found that the MJO is stronger and more likely to propagate across the MC in the QBO easterly (QBOE) phase than the QBO westerly (QBOW) phase defined at 50hPa, and such QBO impacts on the MJO are only significant in the boreal winter season. Also, the MJO is the only one among the convectively coupled equatorial waves (CCEWs) that is affected by the QBO phase in the observations (Sakaeda et al., 2020). Many hypotheses have been proposed to understand the QBO-MJO connection since its discovery including the cloud-radiative feedback theory involving the QBO-induced changes in high clouds around the tropopause (Son et al., 2017), the tropopause instability theory where the MJO-induced, wave-like temperature disturbances in the upper troposphere and lower stratosphere (UTLS) are emphasized (Hendon and Abhik, 2018), the QBO wind shearing effects on deep tropical convection (Collimore et al., 2003), as well as the impacts from extratropical wave forcing (Hood and Hoopes, 2023) and sea surface temperature changes (Randall et al., 2023). However, the physical mechanisms behind the observed QBO-MJO connection remain poorly understood and debated.

One great challenge to understand the observed QBO-MJO connection stems from climate models' failures in representing this relationship. Lim and Son (2020) analyzed four Coupled Model Intercomparison Project phase 5 (CMIP5) models and found that the QBO-MJO connection is not represented there. Kim et al. (2020) reached similar conclusions using data from the 30 Coupled Model Intercomparison Project phase 6 (CMIP6) models. The lack of QBO-MJO connection in these studies is likely the result of a biased QBO in the models as the simulated QBO is usually too weak in the UTLS levels. In turn, these studies motivated further attempts to capture the QBO-MJO connection in climate models with the observed QBO variability nudged into the model stratosphere. An ocean-atmosphere coupled model from NASA was firstly used in Martin et al. (2021) with a nudged stratosphere towards the observations. However, the model failed to capture the QBO-MJO connection. In Martin et al. (2023), four state-of-the-art climate models were employed relaxing their stratosphere towards the reanalysis, but they also failed to capture the QBO-MJO connection. It is suggested by these two studies that the simulated MJO convection is not deep enough compared with observations, which causes the QBO's failure to modulate the MJO through UTLS stability. However, using a cloud-resolving regional model, Martin et al. (2019) reproduced the observed QBO impacts on MJO convection in a case study, followed by two more successful MJO case studies of the QBO-MJO connection using the numerical models (Back et al., 2020; Huang et al., 2023). It is also noteworthy that the QBO-MJO connection is represented in the subseasonal-to-seasonal weather forecast system by different MJO predictability and prediction skills conditioned by the QBO phase, although the connection is weaker than in observations (Marshall et al., 2017; Lim et al., 2019; Kim et al., 2019; Wang et al., 2019; Martin et al., 2020).

The Atmospheric Processes And their Role in Climate (APARC, previously "SPARC") QBO initiative (QBOi, Anstey et al., 2022) is a community-driven activity by global climate modeling centers. It aims to improve the fidelity of tropical stratospheric variability in general circulation and Earth system models by conducting coordinated numerical experiments and analysis (Butchart et al., 2018). The QBO-MJO connection was examined in nine models participating phase 1 of the QBOi project with internally generated QBO, and no significant connection between QBO and MJO was found (Elsbury et al., 2026). In phase 2 of the QBOi project (Anstey et al., 2026), the participating climate models conducted a series of experiments including the simulations where the zonal wind in the model stratosphere over the tropics is nudged towards the



observations (Exp1-ObsQBO simulations, here and after). The QBOi phase 2 simulations are conducted in an Atmospheric Model Intercomparison project (AMIP) style with prescribed sea surface temperature and sea ice from the observations as the forcing. Compared with the simulations with a free stratosphere, the QBO variations in the Exp1-ObsQBO simulations are much closer to the observations with the zonal wind biases largely corrected (Andrews et al., 2026).

This study diagnoses the potential connection between the nudged QBO and the internally simulated MJO in the Exp1-ObsQBO simulations by 12 participating models around the globe. Especially, compared with the previous studies using model simulations with a nudged stratosphere (Martin et al., 2021, 2023), the Exp1-ObsQBO simulations by the QBOi phase 2 project include more models from global modeling centers, providing an opportunity to broaden our understanding of the model capability in QBO-MJO connection representation with the model stratospheric biases corrected. According to the available daily output variables from the QBOi phase 2 experiment, this study mainly focus on the tropopause instability and cloud-radiative feedback theories for diagnostics.

2 Data and Method

2.1 Model and reanalysis dataset

To investigate the QBO-MJO connection, we employed the Exp1-ObsQBO simulations from the phase 2 of the QBOi project. In these simulations, the zonal-mean zonal wind in the stratospheric levels of the model are relaxed towards that in the European Centre for Medium-Range Weather Forecast Reanalysis version 5 (ERA5, Hersbach et al., 2020), which is done through a zonal-mean or full-field nudging in the model levels from 100 hPa to 5 hPa. The nudging intensity is controlled by the nudging timescale where a stronger nudging is applied with a shorter nudging timescale. The nudging is conducted with a timescale of 5 days in the model levels from 70 hPa to 10 hPa, and it is weakened downward and upward with the nudging timescale gradually increasing to infinity at the levels above 5 hPa or below 100 hPa. Also, the stratospheric nudging is only conducted in the tropics with the nudging timescale being 5 days from 10°S to 10°N and gradually increasing to infinity at latitudes higher than 20°. Details of the nudging protocol for the Exp1-ObsQBO simulations in phase 2 of the QBOi project can be found in Anstey et al. (2026). We focus on nudged simulations in this study, given that previous studies have consistently shown that the QBO-MJO connection is missing in free-running climate model simulations (e.g., Kim et al., 2020). Twelve models employed in this study are shown in Table 1. The ensemble members along with the nudging type and the daily variables used for investigations are also given there. Due to the lack of daily wind variables, one ensemble member from E3SMv2 and the entire LMDz ensemble are excluded from the analysis based on the realtime multivariate MJO index (RMM index, Wheeler and Hendon, 2004).

We used the model outputs from 1980 to 2020 for our diagnostics. They are compared against the daily wind field from the ERA5 reanalysis dataset, the daily outgoing longwave radiation (OLR) from National Centers for Environmental Information of the National Oceanic and Atmospheric Administration (Lee, 2025) in the same years, and the daily precipitation from the version 1.3 of the Global Precipitation Climatology Project (GPCP; Huffman et al., 2001) from 1997 to 2020. These



Table 1. Daily data availability in the years of 1980 to 2020 from the 12 QBOi phase 2 climate models for their simulations with a nudged stratosphere towards the observations (Exp1-ObsQBO). The nudging type is indicated as zonal-mean (ZM), in which case only the zonal-mean zonal wind is nudged, or full-field (FF). The daily variables used in this study include daily precipitation, OLR, zonal wind at 850 hPa (u850), and zonal wind at 200 hPa (u200).

Model	Ensemble member	Nudging type	Unavailable daily variables
BCC-CSM2-MR	r1i1p1f1-r3i1p1f1	ZM	none
CAS-ESM	r1i1p1f1-r1i3p1f1	ZM	none
CESM2	L83_cam6.001-003	ZM	none
E3SMv2	r1i1p1f1-r3i1p1f1	FF	u200 and u850 in r1i1p1f1
EC-Earth3	r1i1p1f1	FF	none
ESM4	r1i1p1f1-r3i1p1f1	FF	none
HadGem3GA7-1	r1i1p1f1-r3i1p1f1	ZM	none
LMDz	Exp1-Exp3	ZM	u200
GRIMs	r1i1p1f1	ZM	none
MIROC6.1_p1	r1i1p1f1-r3i1p1f1	ZM	none
MIROC6.1_p2	r1i1p2f1-r3i1p2f1	ZM	none
MRI-ESM2-0	r1i1p1f1-r3i1p1f1	ZM	none

105 variables are interpolated onto the same 2.5° by 2.5° horizontal grids for the observations and model outputs before running the diagnostics.

2.2 Methods

The QBO phase in this study is defined at the 50-hPa level using the season-averaged and zonal-mean zonal wind around the equator (10°S-10°N) as the QBO index. When the QBO index is below its mean minus half of its standard deviation, a QBOE
 110 season is assigned. Similarly, a QBOW season is defined as when the QBO index is above its mean plus half of its standard deviation.

The MJO-related variations are extracted by applying a 2-dimensional filtering at the zonal-wavenumber-frequency space to retain only the 20-100-day, eastward-propagating variations with a zonal wavenumber of 1 to 10, unless specified. The MJO behaviors are also measured by the RMM index (Wheeler and Hendon, 2004), which are calculated using the daily OLR, zonal
 115 wind at 200 hPa (u200) and 850 hPa (u850) from the model outputs and observations. The explained variance percentages for the first two empirical orthogonal functions of the RMM indices derived from the observations and model simulations as well as their spatial patterns are given in Appendix.A. The significance for the composite analysis in this study is tested using a bootstrap test with 1000 times of sampling and replacements. For the linear correlation analysis, their correlation coefficients are also tested with a 95% confidence level.

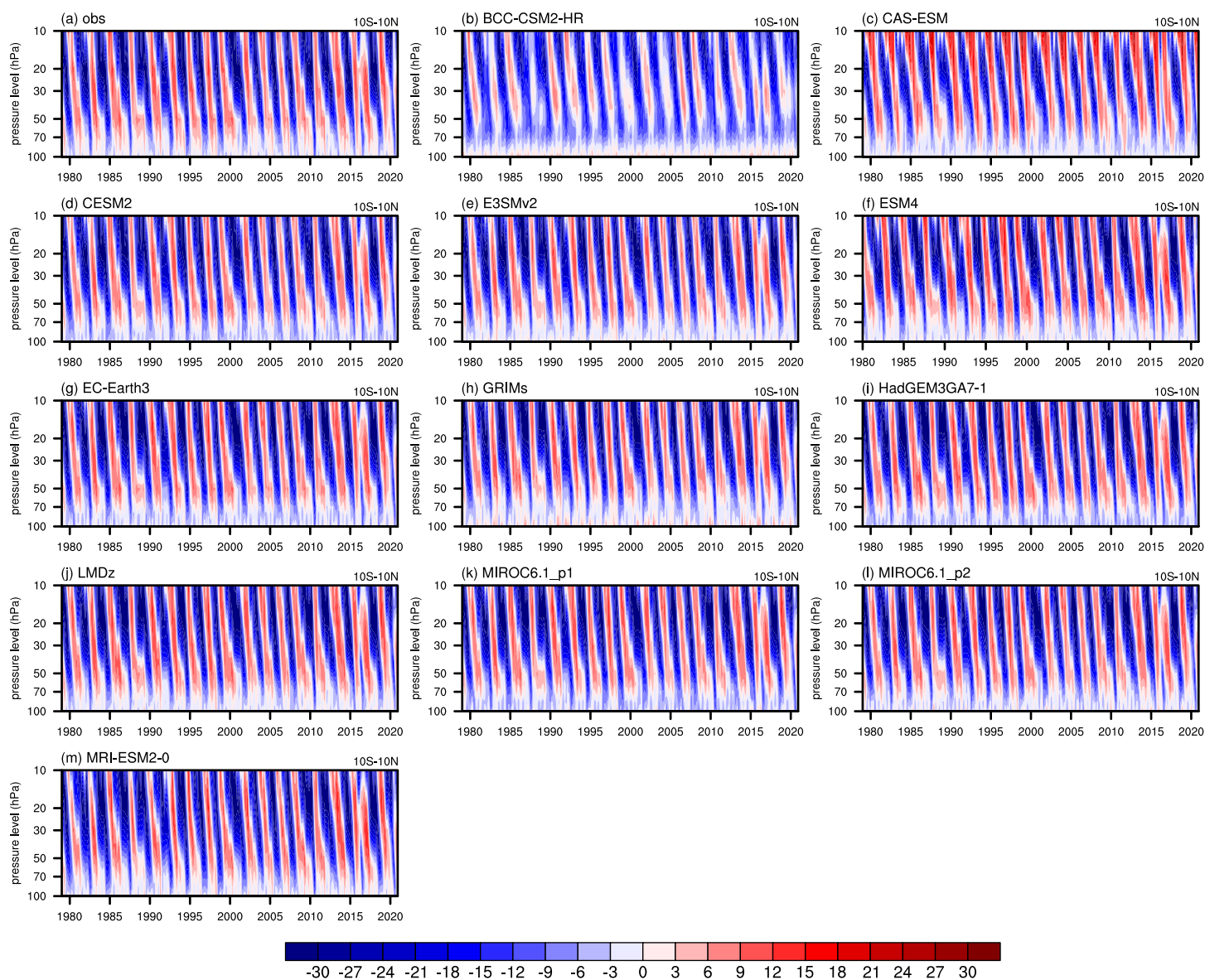


Figure 1. Hovmöller diagrams for the monthly zonal wind averaged around the equator (10°S - 10°N) in (a) observations, and (b)-(m) Exp1-ObsQBO simulations by the QBOi phase 2 models with their stratosphere nudged towards the observations in the tropics.



120 3 Results

3.1 QBO in the Exp1-ObsQBO simulations

The QBO in Exp1-ObsQBO simulations is examined at the model stratospheric levels in the tropics to verify the zonal-mean nudging performance for the zonal wind. The Hovmöller diagrams of the monthly zonal wind averaged from 10°S to 10°N in the observations and Exp1-ObsQBO simulations are given in Fig.1. The stratospheric nudging leads to a realistic QBO representation in these simulations with a downward propagation of the wind shear from higher to lower stratosphere and the wind shear phase generally follows that in the observations. The only exception is the Exp1-ObsQBO simulation by BCC-
125 CSM2-MR where the simulated QBO wind is skewed towards the easterly phase. In the lower stratosphere below 70 hPa, where the nudging intensity gradually decreases downward, more deviations from the observations with weaker QBO variations are seen for the zonal-mean zonal wind around the equator in Exp1-ObsQBO simulations.

130 As both the QBO wind and its modulation of the temperature could be important to build the connection between QBO and MJO, their vertical structure differences in the December-January-February (DJF) seasons between QBOE and QBOW phase are shown by Fig.2. In observations, the strong negative wind anomalies are centered around 50 hPa in the tropics in the QBOE DJF season, overlain by positive wind anomalies at the levels above. The QBOE wind pattern leads to cooler anomalies in the UTLS below 50 hPa, which reduces the tropopause stability (Hendon and Abhik, 2018), promotes the high cloud formation (Son et al., 2017), and enhances the seasonal MJO amplitude. As suggested by Fig.2b, the QBO wind anomalies are well represented in the tropics through nudging across the Exp1-ObsQBO simulations, while more biases are found at higher latitudes (Fig.2d-o) such as the underestimated westerly at 20 hPa and above from 20°N. The coherent temperature changes by QBO wind shear is captured in the simulations although the cooling effects around the tropical UTLS induced by the QBOE phase are slightly underestimated across the models (Fig.2c). Same as the QBO wind, the QBO temperature anomaly biases
135 are also larger at higher latitudes (Fig.2d-m).
140

To summarize, the QBO wind variation is well represented in the Exp1-ObsQBO simulations with a stratospheric nudging in the tropics. For QBO temperature, however, more biases are found in the model. Although the models correctly capture the negative temperature perturbations by the QBOE phase above the tropical tropopause, which is vital to build the QBO-MJO connection in the model through tropopause instability (Hendon and Abhik, 2018) and the cloud-radiative feedback (Son et al.,
145 2017) mechanisms, these temperature differences are about one half to two thirds of that in observations.

3.2 MJO representation

As no nudging is conducted in the troposphere for the Exp1-ObsQBO simulations, the QBOi phase 2 model performance in simulating the tropical convection varies in the boreal winter season (November to April). The simulated season-mean convection strength over the tropical Indo-Pacific region is shown by the averaged OLR maps (Fig.3). The observations exhibit intense convection around the MC as evidenced by the lower OLR in that region which extends both westward into the deep IO and eastward into the Pacific (Fig.3a). Over the Pacific, convective activity splits into two branches over the Northern and Southern hemisphere, known as the intertropical convergence zone (ITCZ, Waliser and Gautier, 1993) and South Pacific
150

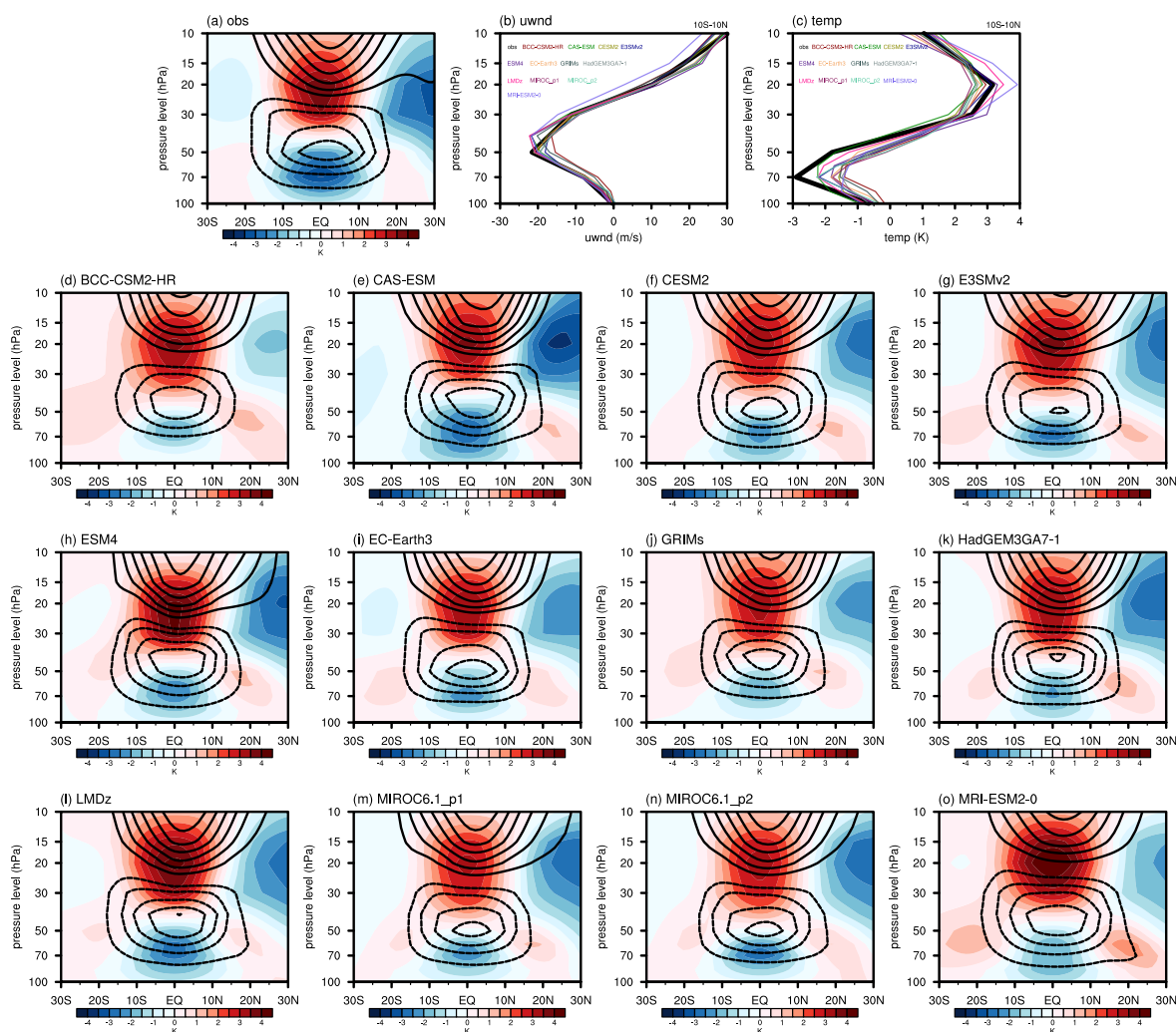


Figure 2. Meridional structures of the global mean temperature (shadings) and zonal wind (contour lines) difference in the stratosphere between the December-January-February seasons with a QBOE and QBOw phase for (a) observations, and (d)-(o) Exp1-ObsQBO simulations by the QBOi phase 2 models. The interval of contour line is 5 m/s with zero lines omitted. The vertical profiles for the zonal wind and temperature differences averaged between 10°S and 10°N are given in (b) and (c), respectively, with the observations denoted by the thick black lines and model results denoted by the colorful lines.



convergence zone (SPCZ, Vincent, 1994). The same spatial pattern is identified across Exp1-ObsQBO simulations, but there are some common biases in the QBOi phase 2 models compared with observations (Fig.3b-m), such as an overall underestimation centered around the MC. This is indicated by the systematically higher season-mean OLR over the MC and over the eastern IO. Exceptions are GRIMs, MIROC6.1_p1, MIROC6.1_p2, and MRI-ESM2-0 since negative OLR biases are seen over the IO basin, suggesting the simulated convection is overly strong. Over the Pacific Ocean (PO), GRIMs, MIROC6.1_p1, and MIROC6.1_p2 also overestimate the convection strength across the tropical basin. For ITCZ and SPCZ, CAS-ESM, E3SMv2, EC-Earth3, HadGem3GA7-1, LMDz, and MRI-ESM2-0 underestimate their seasonal-mean strength.

The spatial patterns for the biases in the MJO convective variation generally follows that for the boreal-winter-mean convection biases. Figure 4 shows the MJO-filtered (20-100-day, and eastward-propagating with zonal wavenumber of 1-10) OLR standard deviation maps in the boreal winter season from the observations and from the QBOi phase 2 models. Strong MJO convective variations are found over the eastern IO, the southern sea surface of the MC, as well as over the WP in the Southern Hemisphere overlapping the SPCZ from the observations, representing the robust eastward propagation of the MJO convection in the boreal winter season. In QBOi phase 2 models, however, the MJO convective variation in Exp1-ObsQBO simulations is weaker than that in the observations around the MC, following the underestimation of the season-mean convection over the same locations. The negative MJO convective variance biases are largest in BCC-CSM2-MR, CAS-ESM, and MIROC6.1. Note that although the spatial patterns of MJO convective variance biases generally resemble those of the boreal-winter mean convection biases, the bias magnitudes are not necessarily correlated across models. For example, EC-Earth3 shows relatively small biases in MJO convective variance, while it exhibits substantial biases in the season-mean convection over the MC. This may reflect the commonly discussed trade-off between the mean state simulation and MJO simulation in climate models as noted by many previous studies (e.g., Kim et al., 2012; Jiang, 2017). GRIMs is unique among the QBOi phase 2 models as the model simulates extraordinarily stronger MJO convective variances in the subtropics, over the western IO, and central PO.

The tropical convective variability in the QBOi phase 2 models are more comprehensively evaluated by the zonal-wavenumber-frequency power spectrum analysis for the daily precipitation anomalies around the equator (15°S-15°N) following Wheeler and Kiladis (1999). The power spectra for the symmetric and anti-symmetric part of the precipitation are given by Fig.5 and Fig.6, respectively. They reflect the model performance in simulating the convectively coupled equatorial waves (CCEWs) including the MJO. In the power spectrum for the symmetric part of the observational precipitation (Fig.5a), anomalous peaks are identified for the convectively coupled Kelvin wave which propagates eastward with positive zonal wavenumbers and with frequencies higher than 0.05. The eastward-propagating MJO is also seen in the domain with the zonal wavenumber of 1 to 5 and frequencies lower than 0.05 per day. At the same timescale but with negative zonal wavenumbers are the power peaks contributed by the westward-propagating equatorial Rossby waves. Anomalous power peaks are also found at timescales shorter than 3 days for the westward-propagating inertial gravity (IG) waves. QBOi phase 2 models have a reasonable simulation of the equatorial Rossby wave except HadGEM3GA-1 where the Rossby wave power peak is relatively weaker. All models exhibit an overly weakly Kelvin wave. EC-Earth3 and HadGEM3GA7-1 are the models with the smallest biases for Kelvin wave. As demonstrated by previous studies (e.g, Liu and Wang, 2013, 2016), the accurate representation of the Kelvin wave is important for the simulation of boreal-winter MJO in the models. Indeed, the MJO peaks in the QBOi phase 2 models are

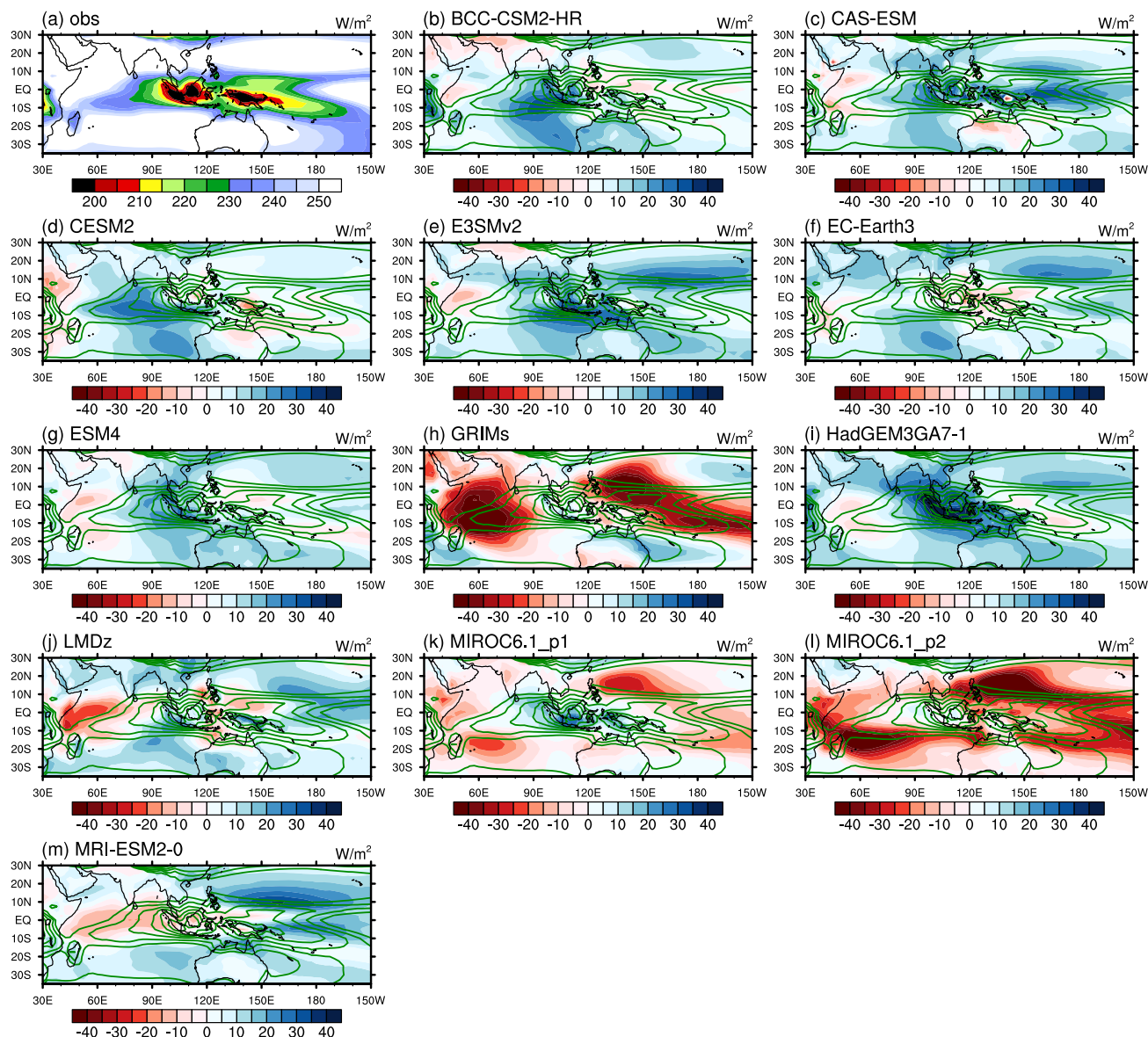


Figure 3. Seasonal mean maps of the OLR in the boreal winters (November to April) for (a) observations, and (b)-(m) model biases from the observations (shadings) for the Exp1-ObsQBO simulations. The contour lines in (b)-(m) denote the observational baseline which starts at 200 W/m^2 with an interval of 5 W/m^2 .

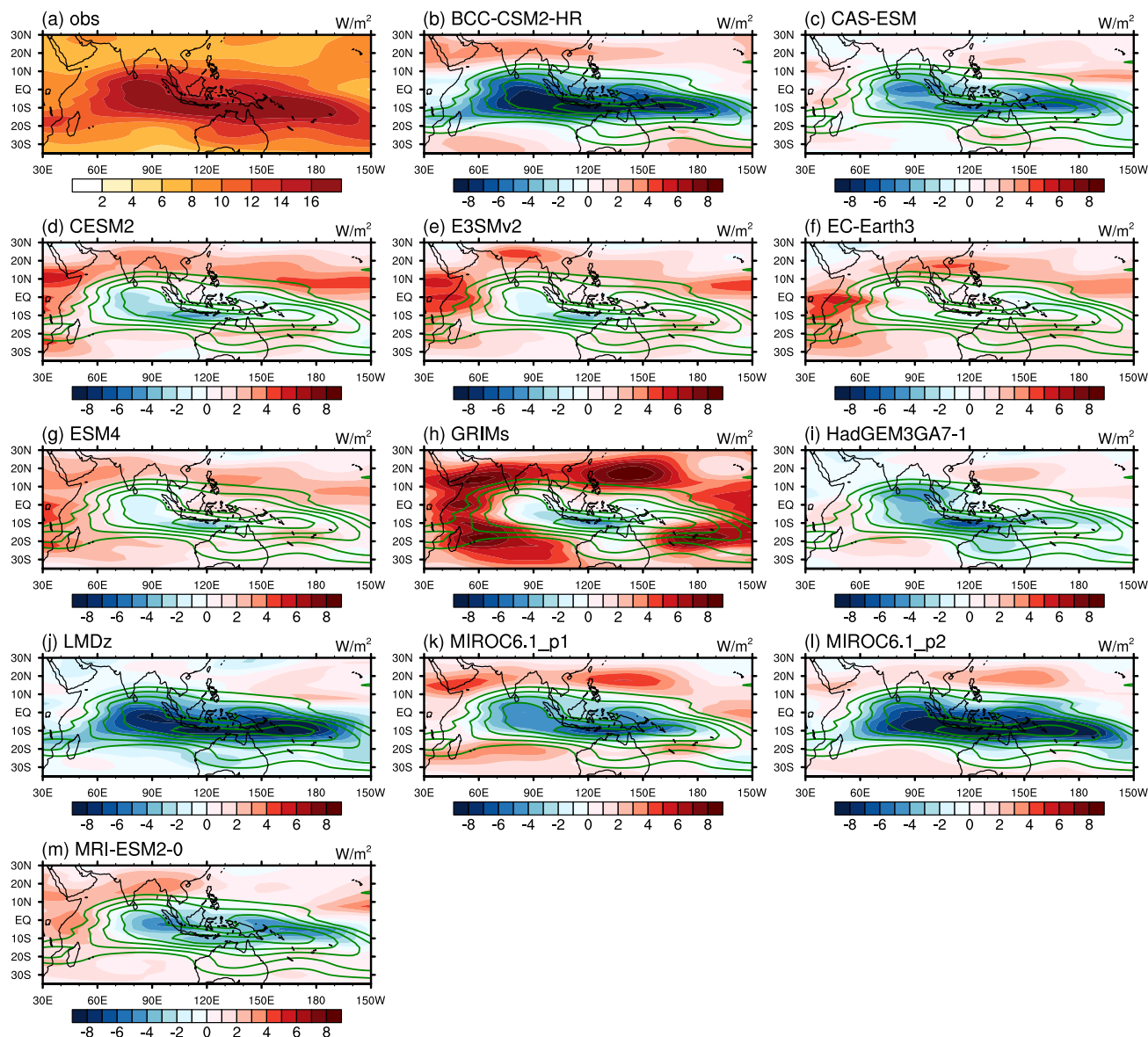


Figure 4. Maps for the MJO-filtered (20-100-day, and eastward-propagating with zonal wavenumber of 1-10) OLR standard deviation in the boreal winter seasons for (a) observations, and (b)-(m) model biases from the observations (shadings). The contour lines in (b)-(m) denotes the observational values starting from 10 W/m^2 with an interval of 2 W/m^2 .

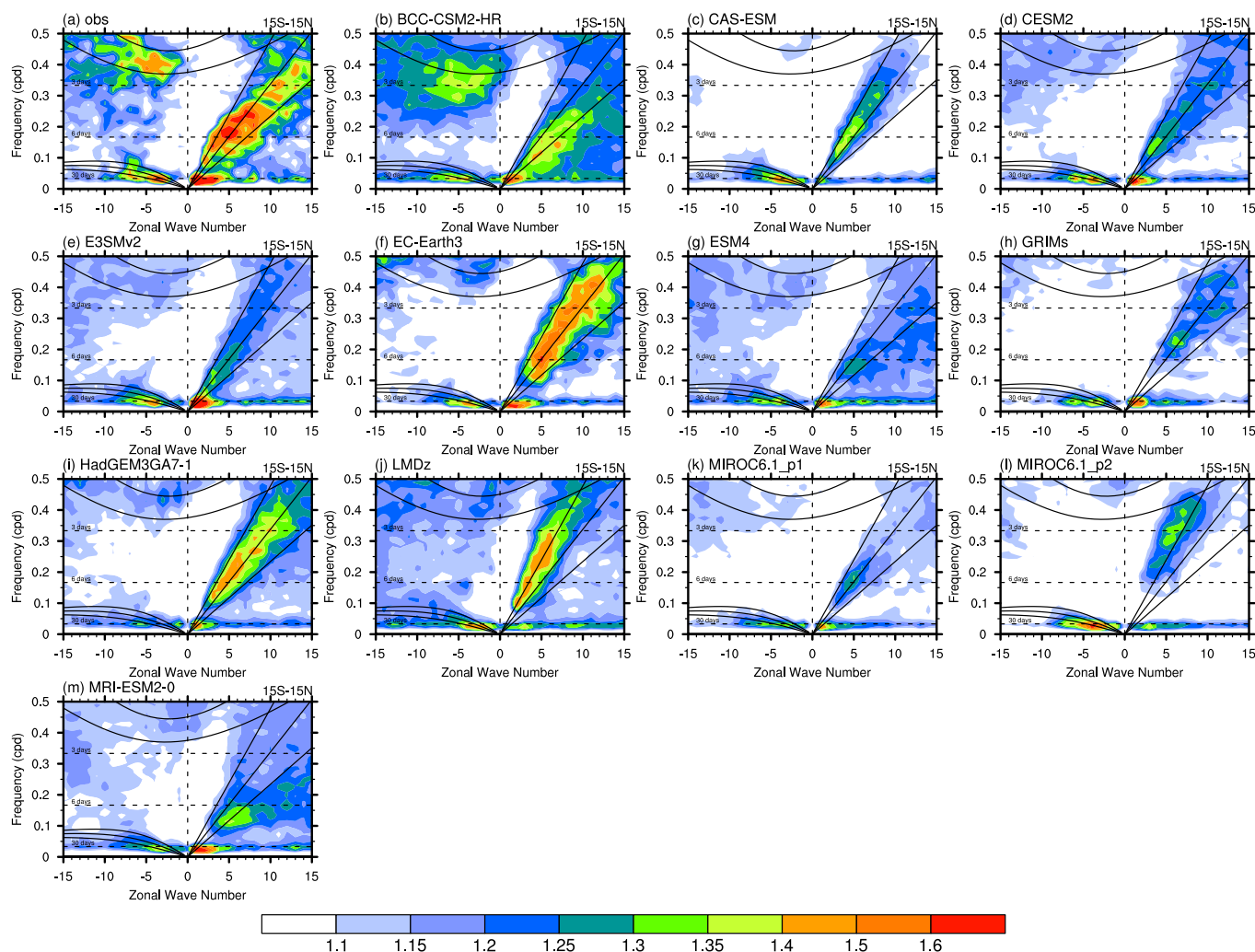


Figure 5. Zonal-wavenumber-frequency power spectrum analysis for the symmetric part of the precipitation around the equator ($15^{\circ}\text{S}-15^{\circ}\text{N}$) in the boreal winter season from (a) observations, and (b)-(m) models. The ratio of the raw spectrum to its background is shown.

also too weak and with smaller zonal wavenumbers compared with observations, in agreement with the underestimated MJO convective variations over the Indo-Pacific region (Fig.4b-m). For the power spectrum associated with the anti-symmetric part of the equatorial precipitation, strong signals of the mixed-gravity Rossby (MRG) waves are seen in the observations with both eastward and westward propagation (Fig.6a). However, most QBOi phase 2 models miss the associated power peaks for the MRG wave especially at smaller zonal wavenumbers, except CESM2, EC-Earth3, and GRIMs.

In summary, unlike the adequate representations of the stratospheric QBO in the Exp1-ObsQBO simulations due to nudging, the freely evolving tropical convective variability in the models are more biased from the observations. The simulated MJO con-

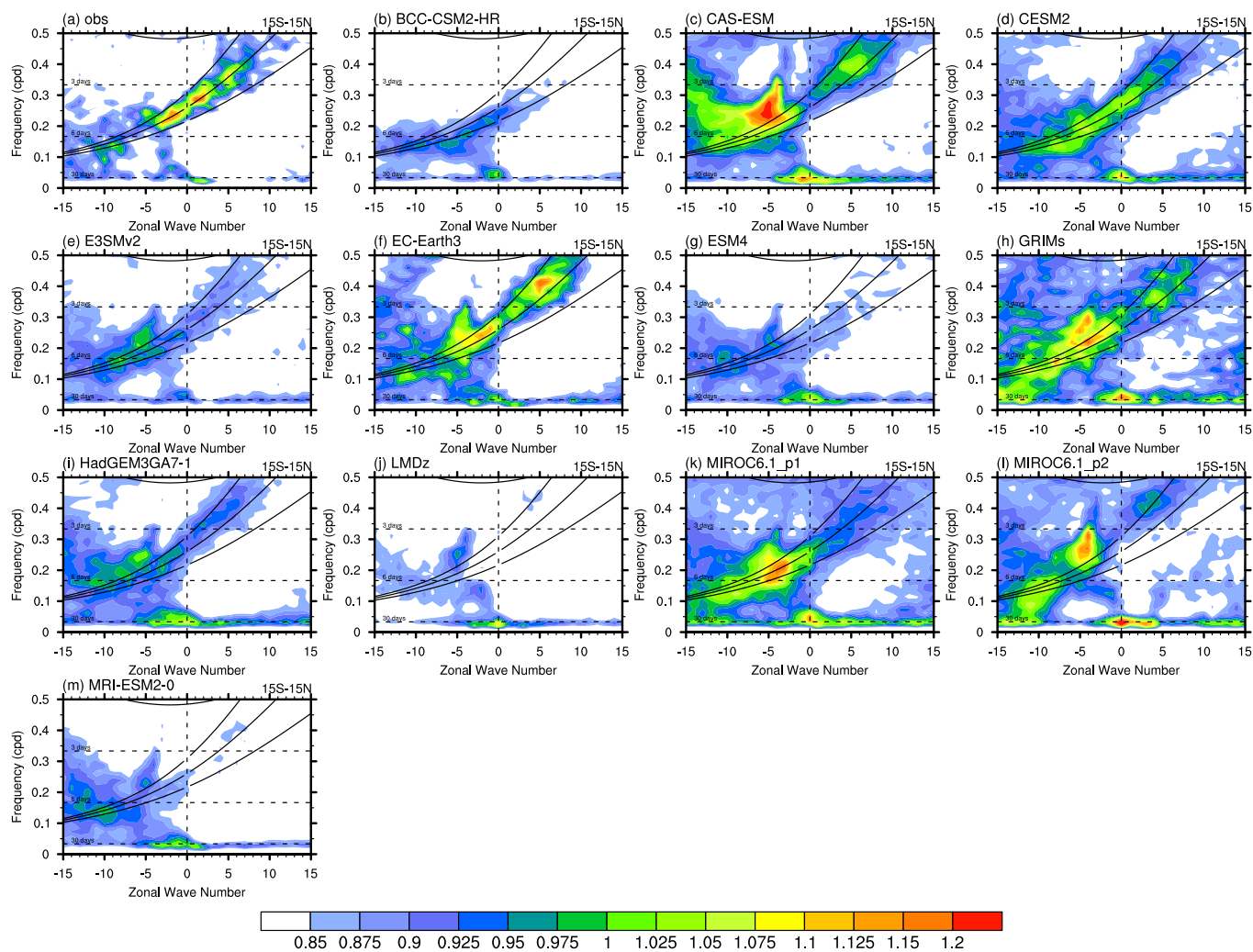


Figure 6. Same as in Fig.4 but for the anti-symmetric part of the equatorial precipitation.



195 vective variation in these models are generally too weak around the MC, following the overly weak season-mean convection at the same locations in the boreal winters. The overly weak MJO convection is also reflected by the zonal-wavenumber-frequency power spectrum analysis of the daily precipitation anomalies associated with the underestimation of convectively coupled Kelvin waves by all models. CESM2, E3SMv2, EC-Earth3, and ESM4 are the models with a relatively smaller underestimation of the MJO convective variations. Among them, EC-Earth3 is the top model in the overall simulation of CCEWs.

200 3.3 Lack of the QBO-MJO connection

Comprehensive diagnostics of the relationship between the stratospheric QBO and MJO are conducted in search for a potential connection between these two modes of variability. The standard deviation of the MJO-filtered OLR anomalies is calculated in DJF, and the differences are made between QBOE and QBOW phase (Fig.7). From observations, significant enhancements in the MJO convective variance are found over the Indo-Pacific region centered around the MC in the Southern Hemisphere, a result of the observed QBO-MJO connection in the boreal winter season (Yoo and Son, 2016; Son et al., 2017). In Exp1-ObsQBO simulation by the QBOi phase 2 participating models, although the observational QBO wind and temperature perturbations are reasonably represented in the stratosphere through nudging (Fig.1 and Fig.2), the simulated MJO is not responding correctly to the stratospheric QBO phase. In most of the models, there are almost no MJO convective variance differences over the Indo-pacific region at different QBO phases. In GRIMs, enhancements are seen over the southern IO and southwestern Pacific (Fig.7h) where the simulated MJO convective variation is unrealistically strong (Fig.4h). However, the robustness of such responses is questionable as the GRIMs simulation only consists of one member (Table 1). Significant MJO convective variance increases are found over the southern MC in MIROC6.1_p2 (Fig.7l), but the increases are very slight. In addition, the DJF-mean MJO convective variances are mostly off the equator in MIROC6.1_p2 (contour lines in Fig.7l). Therefore, it remains questionable whether the slight but significant MJO convective variance increases around the equator in the QBOE phase corresponds to a representation of the QBO-MJO connection in the model, which will be further examined by the RMM-based analysis in the rest of the paper. In EC-Earth3 with the best representations of the MJO and other CCEWs among all models, the QBO impacts on MJO are misrepresented by decreased MJO variances south of the MC in the QBOE phase (Fig.7f).

To better understand the ensemble-spread of the MJO convective variation differences conditioned by the QBO phase in Exp1-ObsQBO simulations, we calculated the member-by-member MJO-filtered OLR standard deviation differences averaged over the Indo-Pacific domain (20°S-5°N, 50°E-170°E) between the QBOE and QBOW DJF seasons (Fig.8) following Kim et al. (2020). None of the members from these models simulates a positive MJO convective standard deviation difference that could exceed its confidence interval, largely lower than the significantly positive differences from the observations. Notably, in EC-Earth3 with the most realistic representations of the stratospheric QBO and tropospheric CCEWs, its averaged difference over the Indo-Pacific domain is around 0.

225 As demonstrated by Son et al. (2017), the observed QBO-MJO connection exhibits a strong seasonality that only in the boreal winter seasons the MJO becomes stronger and more likely to propagate across the MC in the QBOE phase. We extend the examination of the potential connection between the QBO and MJO in the Exp1-ObsQBO simulations to all the seasons around the year in case the models misrepresent the QBO-MJO connection seasonality that it is found in other seasons. Figure

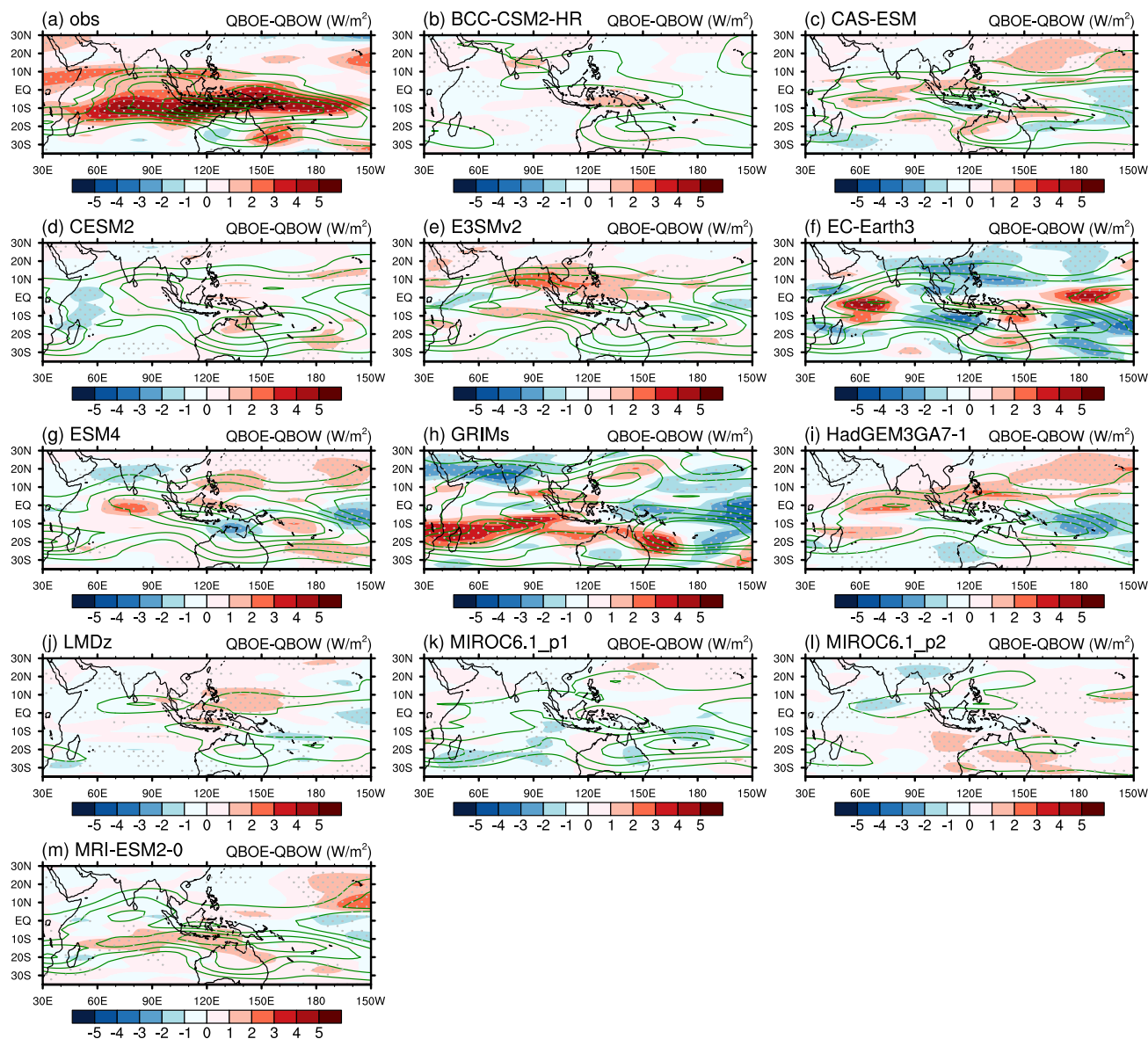


Figure 7. The difference maps for the MJO-filtered OLR standard deviation between the DJF seasons with QBOE and QBOW phase (shadings) with the all-season-mean denoted by the contour lines in the (a) observations, and (b)-(m) QBOi phase 2 models. The significant differences at 95% confidence level through the bootstrap test with 1000 times of sampling and replacements are stippled.

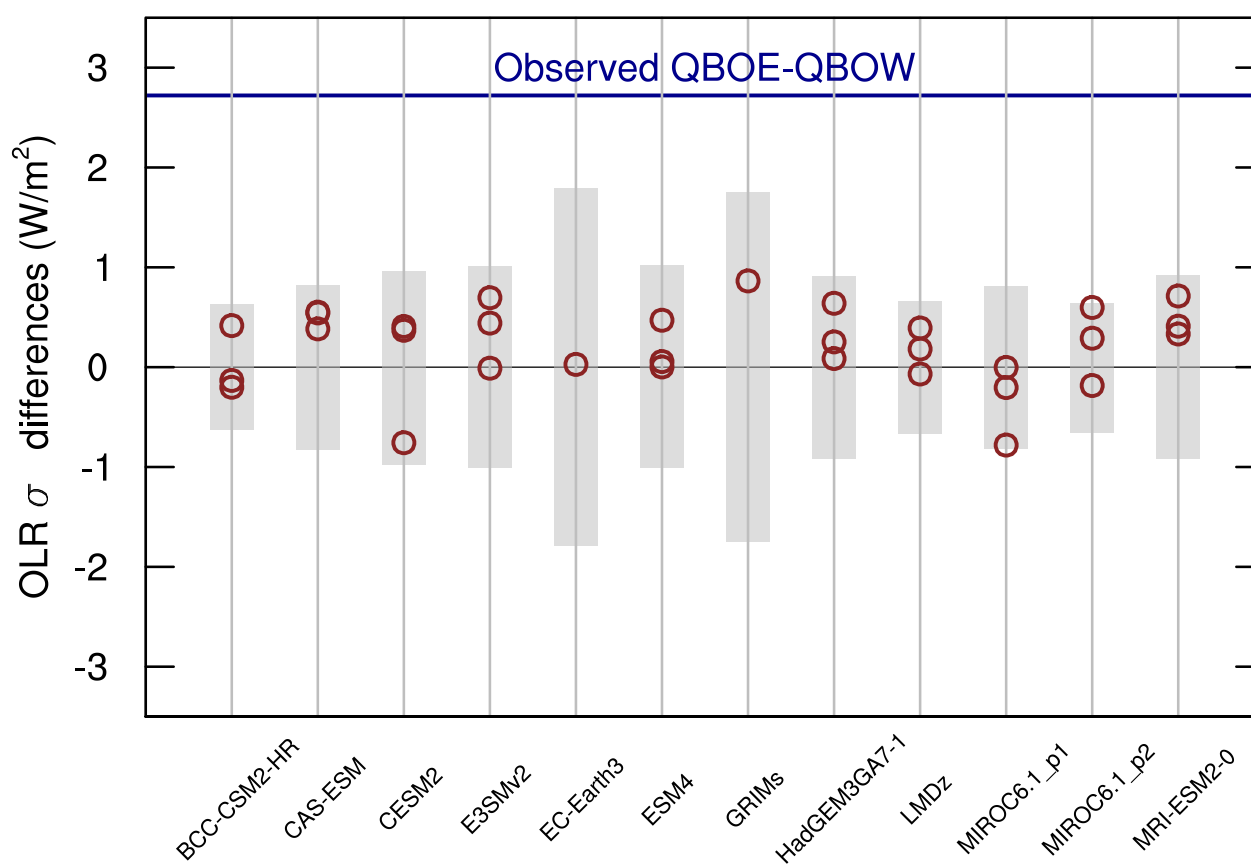


Figure 8. Ensemble spread of the OLR standard deviation differences over the Indo-Pacific domain (20°S-5°N, 50°E-170°E) between the QBOE DJF and QBOW DJF seasons from the Exp1-ObsQBO simulations by various QBOi phase 2 models. Each circle represent an individual member from the simulations. The gray shadings denote the 95% confidence interval which is calculated from the bootstrap tests with 1000 times of sampling using all members for each model and with replacements. The difference value from the observations is marked by the blue line.



9 gives the correlation coefficients between the three-month-mean zonal wind at the 50 hPa level (u_{50}) and the three-month-
230 mean RMM amplitude. From the observations, in agreement with the QBO-MJO connection seasonality, there are significantly
negative correlation coefficients only in the November-December-January (NDJ), DJF, and January-February-March (JFM)
seasons. In other seasons, the correlation coefficients fail to exceed the 95% confidence interval. In most QBOi phase 2 models,
the correlation coefficients from all members in the Exp1-ObsQBO simulations stay within the confidence interval across all
seasons. Two members from CAS-ESM and show significantly negative correlation coefficients in the July-August-September
235 (JAS) and August-September-October (ASO) seasons and one of them is with significantly negative correlation coefficients
in May-June-July (MJJ) and June-July-August (JJA) seasons. However, such significant connection is not seen in the other
CAS-ESM member. Similarly, one MIROC6.1_p2 member shows significantly negative correlation coefficients from the MJJ,
JJA, and JAS seasons, but the other two members do not agree with it. Significantly negative correlation coefficients are
also found in DJF and JFM seasons in the simulation by one member of E3SMv2 and in the NDJ and DJF seasons by one
240 MIROC6.1_p2 member, respectively. But they are disagreed by the model members where the correlation coefficients between
the season-mean QBO index and RMM amplitude are not significant.

The UTLS is considered critical in many proposed physical mechanisms to explain the observed QBO-MJO connection
such as the wind shear theory (Collimore et al., 2003), the tropopause instability theory (Son et al., 2017; Hendon and Abhik,
2018), and the cloud-radiative feedback theory (Son et al., 2017). The QBO wind and temperature anomalies in the UTLS are
245 adequately represented in the Exp1-ObsQBO simulations through the stratospheric nudging (Fig.2). Although no connections
are found between the simulated MJO and the nudged QBO wind at 50 hPa, it's worth investigating how the QBO wind
anomalies at other vertical levels in the model may interact with the MJO since the weaker MJO convection in the Exp1-
ObsQBO simulations across the QBOi phase 2 models (Fig.4) may require the QBO variations at lower stratospheric levels
to be impacted. Therefore, we extend the QBO-MJO connection analysis in Fig.9 to all vertical levels above 100 hPa in the
250 models and across all three-month seasons (Fig.10). In the observations, significantly negative correlation coefficients originate
as early as in April-May-June (AMJ) at the levels from 10 hPa to 40 hPa. These significant correlation coefficients propagates
downward with seasons till JJA of the next year, superimposed by significantly positive correlation coefficients at the vertical
levels above. Such a pattern is associated with the coherent QBO wind structure across the vertical levels in the stratosphere
along with a downward propagation (Baldwin et al., 2001). However, no significant correlations are found between the QBO
255 wind shear and MJO amplitude at all stratospheric levels across all seasons for QBOi phase 2 models.

To summarize, comprehensive assessments are conducted in search of the potential relationship between the stratospherically
nudged QBO and internally-generated MJO in Exp1-ObsQBO simulations from the QBOi phase 2 models. The assessments
are done across the stratospheric vertical levels and all the seasons around the year. Results show that no significant QBO-MJO
connection is found in any of the participating models.

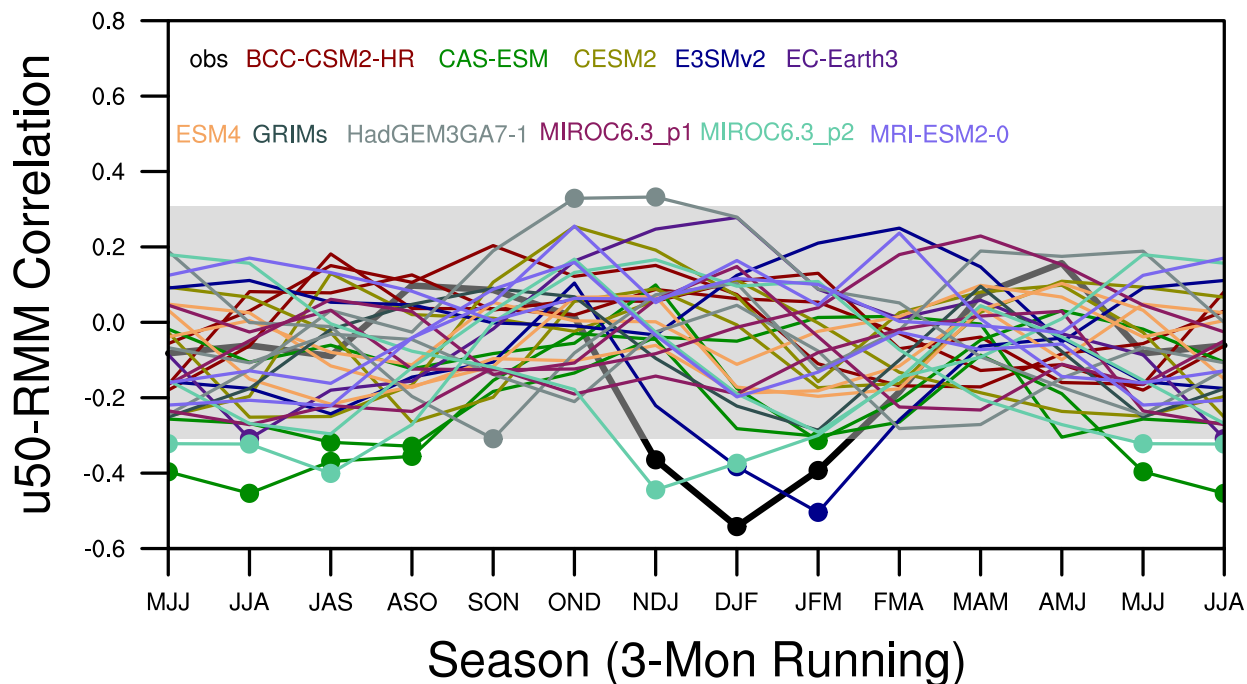


Figure 9. Seasonality of the QBO-MJO connection from the observations and the model results measured by the correlation coefficients between the 3-month-averaged u_{50} and the 3-month-mean RMM amplitude. Each colorful line represents an individual ensemble member. The gray shading denotes the 95% confidence interval of for correlation coefficients and the ones exceeding it are marked by solid dots.

260 4 Conclusions and Discussions

4.1 Conclusions

The phase 2 experiments of the QBOi project provide a valuable opportunity to investigate how the observed connection between the QBO and MJO is represented in the Exp1-ObsQBO simulations with a nudged stratosphere by the 12 participating models. Compared with the previous studies employing single or several North American climate models with stratospheric nudging (Martin et al., 2021, 2023), this study includes more models from other modeling centers around the globe. Also, a tropical-only stratospheric nudging is conducted in the Exp1-ObsQBO simulations. Consequently, the QBO wind anomalies and the coherent temperature responses are induced into the model with the UTLS temperature anomalies underestimated in

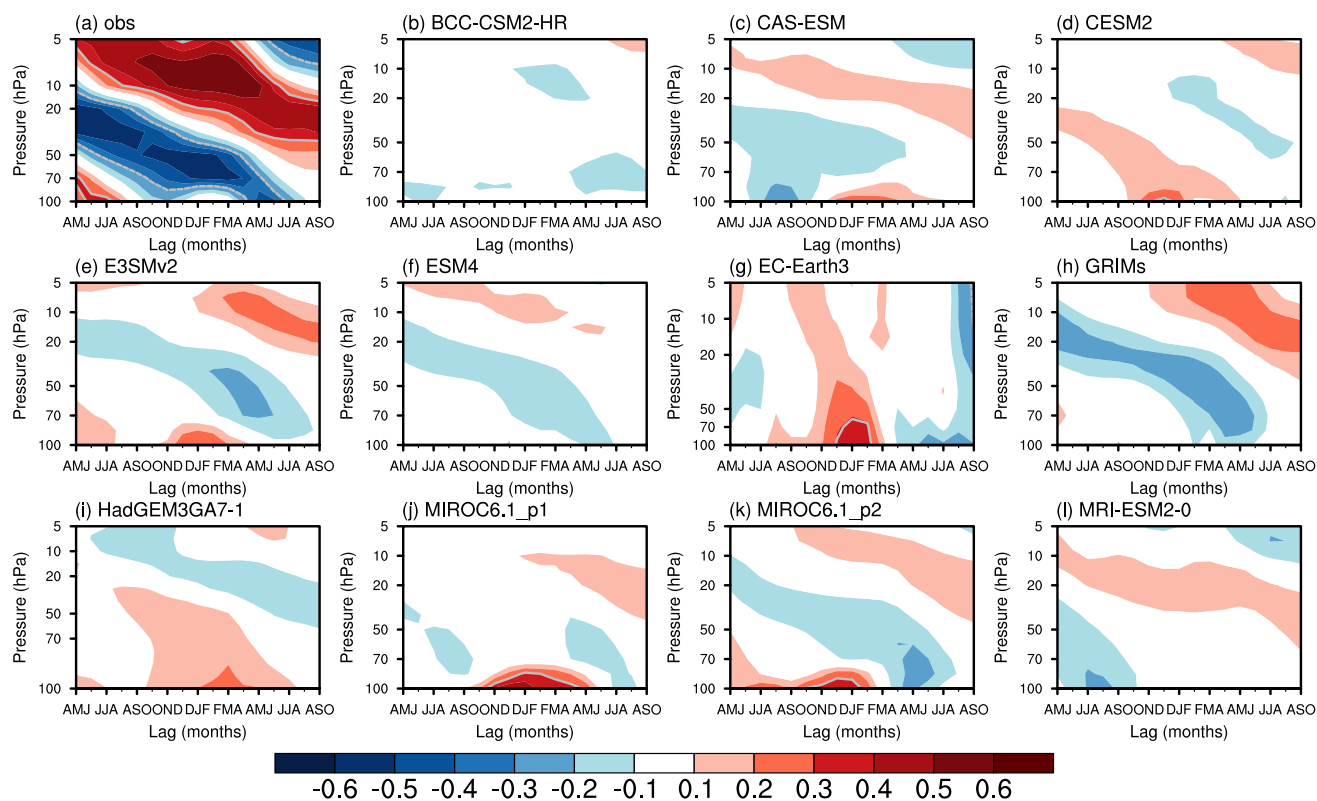


Figure 10. Extension of the seasonality diagnostics in Fig.9 to all vertical levels in the stratosphere. The shadings are the averaged lead/lag correlation coefficients between the 3-month-mean u50 wind and RMM amplitude across the model members. The gray lines represent the boundary for the significant ones at 95% confidence level.



the model (Fig.2). The representations of the QBO through nudging largely correct the widely seen QBO biases in the free simulations by these climate models (e.g., Kim et al., 2020), especially for the overly weak QBO variations around the UTLS. The stratospheric nudging setting along with the AMIP-style forcing setting for the Exp1-ObsQBO simulations in the phase 2 of QBOi project include the QBO impacts on the UTLS wind shear (Collimore et al., 2003), temperature or stability (Son et al., 2017; Hendon and Abhik, 2018), as well as its impacts on the sea surface temperature (Randall et al., 2023).

However, comprehensive diagnostics across the stratospheric levels and the seasons show no significant connections between the simulated MJO and the nudged QBO in these models. Although the weaker UTLS temperature responses by QBO might be a reason, this is more likely a result of the biased MJO in the model. Unlike the nudged QBO in the stratosphere in the Exp1-ObsQBO simulations, the MJO representation varies highly from model to model. All models participating the intercomparison underestimate the MJO convective variation over the MC with the largest underestimations found in BCC-CSM2-MR, CAS-ESM, HadGEM3GA7-1, LMDz, MIROC6.1_p1, MIROC6.1_p2, and MRI-ESM2-0. Among the models participating in the Exp1-ObsQBO simulations, EC-Earth3 exhibits the best performance in the overall simulation of CCEWs. But it also fails to represent a significant QBO-MJO connection.

4.2 Key MJO biases and suggestions for the future work

The lack of a QBO-MJO connection in the QBOi phase 2 climate models with a nudged stratosphere suggests that correction of the model biases in the large-scale QBO variation is not sufficient to capture the QBO-MJO connection. The realistic representation of the MJO physics in the model, such as the sufficient MJO convection depth according to the tropopause instability theory (Hendon and Abhik, 2018) and a reasonable feedback between the MJO cloud and its radiation effects according to the cloud-radiative theory (Son et al., 2017; Martin et al., 2023), is also required to capture the QBO-MJO connection in the model.

Some common MJO biases found across the QBOi phase 2 models participating the Exp1-ObsQBO simulation are likely part of the reasons for the lack of QBO-MJO connection. The first bias is the underestimated MJO convective variance around the MC where the QBO shows the greatest impacts on MJO from the observations. All QBOi phase 2 climate models show negative biases around the MC for the MJO-filtered OLR variance (Fig.4) associated with the strong biases in the season-mean OLR field at the same locations (Fig.3). This is also supported by the derived EOF patterns for the model RMM indices where the combined explained variance from the first two leading EOFs is lower than in observations along with smaller OLR anomalies in the associated spatial patterns. The underestimated MJO convective variation over the MC likely leads to insufficient MJO convection depths in the models (Martin et al., 2021, 2023), which prevents the representation of QBO-MJO connection. The cloud-radiative feedback from MJO convection is also examined. Due to the various parameterization schemes employed in the models, the MJO cloud-radiative feedback is estimated by the linear regression coefficients between the MJO-related precipitation and OLR anomalies. These anomalies are derived by applying a lead/lag linear regression to their daily anomalies against the RMM1 index in each model. Figure 11 and Figure 12 shows the standard deviation maps of the regressed daily OLR anomalies and precipitation anomalies, respectively, from day -20 to day 20. Most models exhibit MJO convective variation over the Indo-Pacific, but it is much weaker than in observations. For all the grid points over the selected

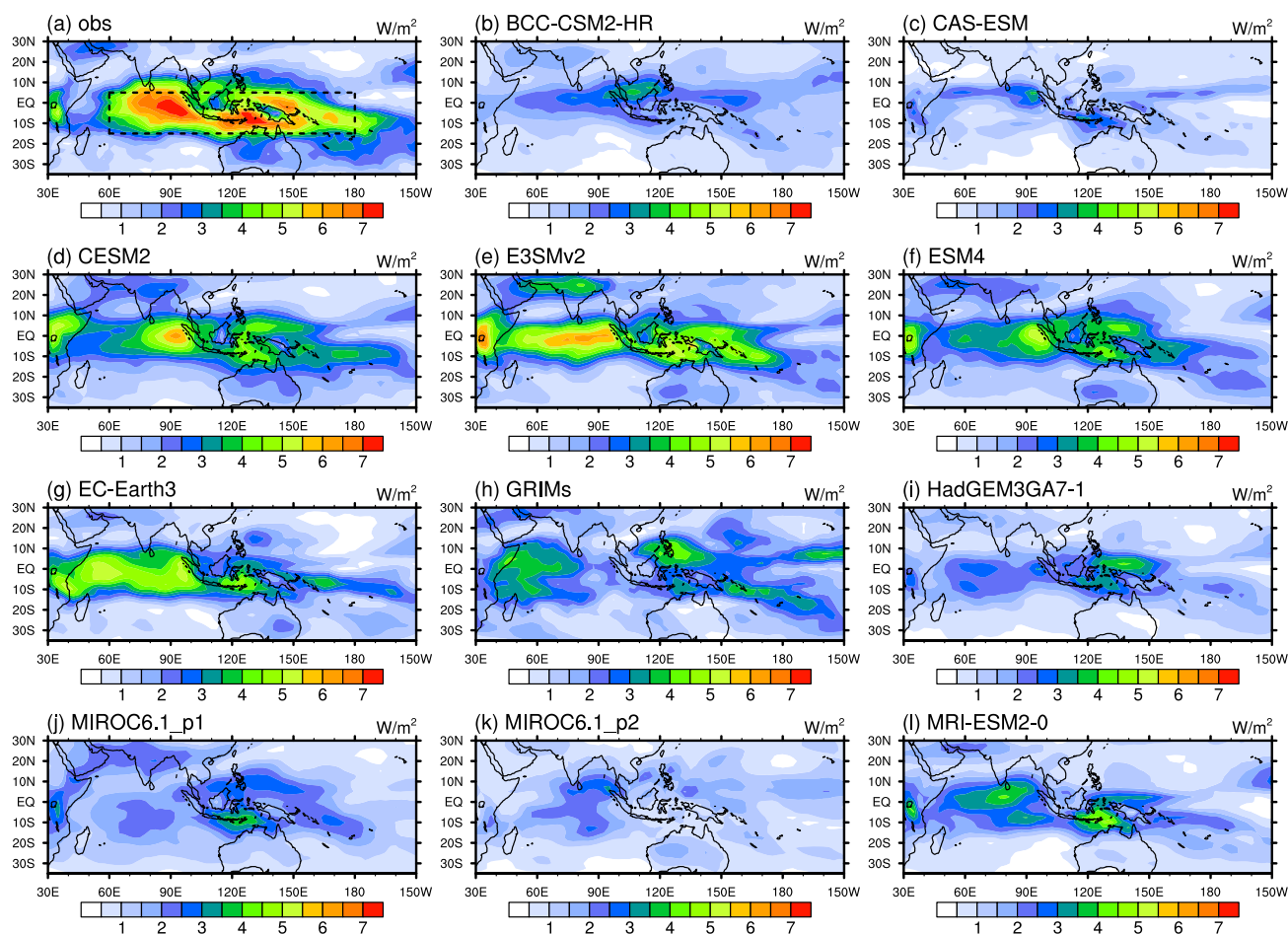


Figure 11. Standard deviation maps of the OLR anomalies lead/lag regressed onto RMM1 from day -20 to day 20 in boreal winter season (a) from the observations in 1997 to 2020, and (b)-(l) from QBOi phase 2 models in 1980 to 2020. The ensemble mean is presented if there are multiple members for the Exp1-ObsQBO simulation according to Table.1. The dashed box in panel (a) corresponds to the Indo-Pacific region (15°S-5°N, 60°E-180°) where the cloud-radiative feedback analysis is done in Fig.13.

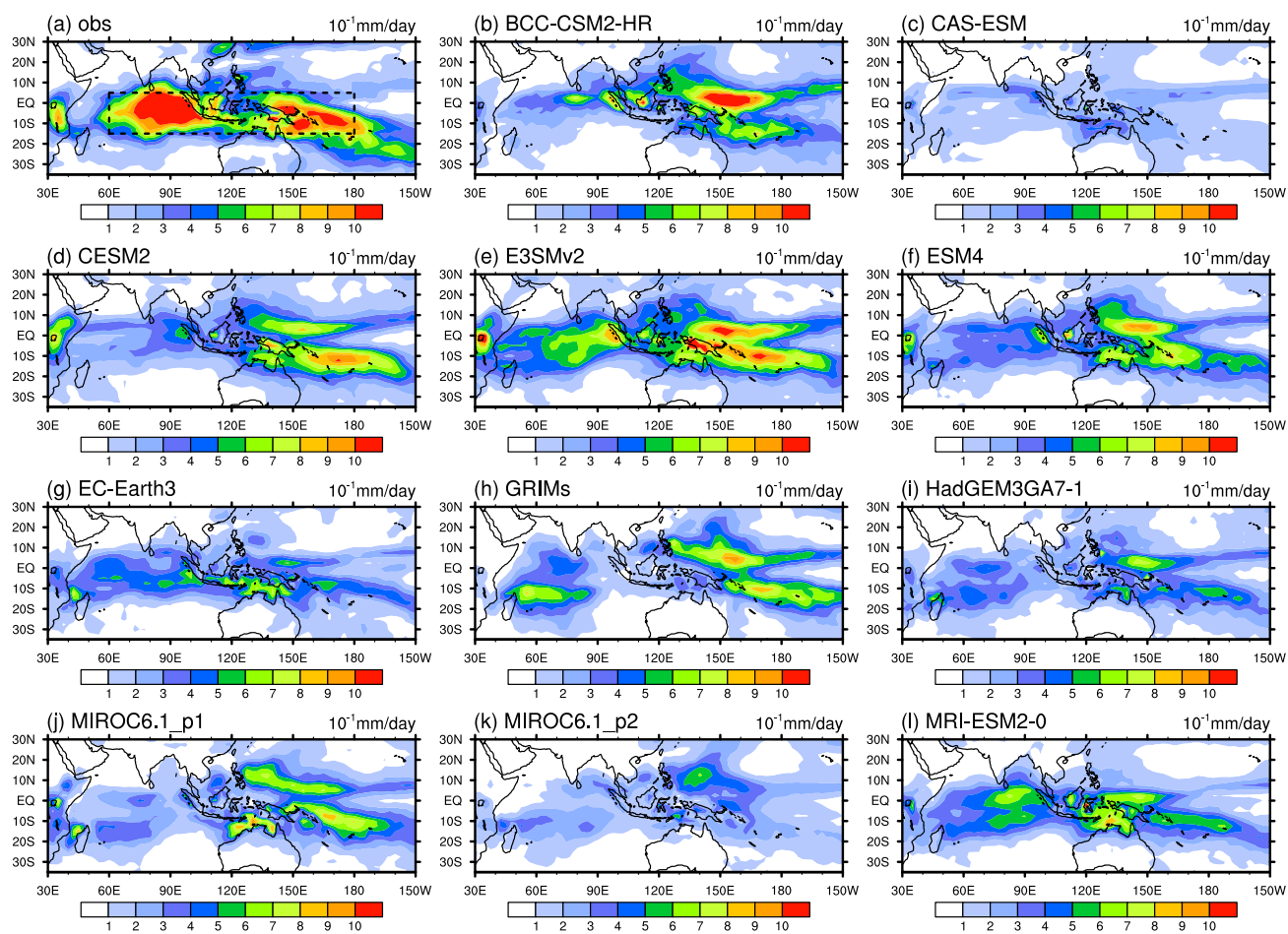


Figure 12. Same as in Fig.11 but for the lead/lag regressed precipitation anomalies.



Indo-Pacific region (15°S - 5°N , 60°E - 180°), the linear regression is conducted between the MJO-related OLR and the latent heat released by precipitation anomalies in each model (Fig.13). The MJO cloud-radiative feedback estimated by the linear regression coefficients between these two variables varies among the QBOi phase 2 models. CESM2, E3SMv2, ESM4, GRIMs, and HadGEM3GA7-1 simulate a cloud-radiative feedback comparable to observations. The MJO cloud-radiative feedback is underestimated by BCC-CSM-HR, MIROC6.1_p1, MIROC6.1_p2, and MRI-ESM2-0, while it is largely overestimated by CAS-ESM and EC-Earth3. However, all QBOi phase 2 models fail to simulate enough strong negative OLR anomalies along with strong positive precipitation anomalies as from observations which are suggested by the dots below -10 W/m^2 for OLR anomalies while above 40 W/m^2 for precipitation latent heating anomalies in Fig.13a. The percentage of these dots is around 4% from observations while nearly missing in all QBOi phase 2 models except EC-Earth3 where the percentage is 2%, in agreement with the insufficient MJO OLR and precipitation variances from these models. This suggests that both a sufficient cloud-radiative feedback and adequately strong OLR and precipitation anomalies are likely necessary to build the QBO-MJO connection in climate models.

Recent advances in MJO dynamics and the theoretical studies on QBO-MJO connection also suggest an important role of the convective and cloud systems at mesoscale or even smaller scales for MJO growth (e.g., Sakaeda and Torri, 2022), propagation (e.g., Liu and Tan, 2025), and its interactions with the QBO (Huang et al., 2025a) through their upscale impacts. These small-scale convective and cloud systems are not well represented by the QBOi phase 2 or other climate models due to their coarse resolution. However, they can be resolved in storm-resolving simulations either by global models (Angulo-Umana et al., 2026) or regional models (Liu and Tan, 2025). This may provide insights for the captured QBO-MJO connection in the cloud-resolving regional model by Martin et al. (2019) and Back et al. (2020).

Therefore, this study suggests that future modeling studies on the QBO-MJO connection should focus more on correcting the MJO biases in the model. In climate models with a relatively coarse resolution, sensitivity experiments are encouraged to test the MJO response to the stratospheric QBO with deepened MJO convection. Future studies may also benefit from the use of storm-resolving models. In storm-resolving simulations, the interactions between resolved multiscale convection and cloud systems within the MJO convective episodes, as well as potential QBO impacts on them should be examined. Along with satellite or in-situ observations at finer spatial and temporal resolutions, better understandings of the coupling processes between the stratosphere and the tropospheric convection in the tropics are likely to be achieved.

Data availability. The QBOi data archive was kindly hosted by the NERC Centre for Environmental Data Analysis (CEDA), UK.

Author contributions. K.H., C-H.P., S-Y.B., J.G-F., H.K., P.L., S.O., J.R., C-C.C., S-W.S., S.Y., Y.L.: Conceptualization of the goals and aims of this analysis. Formal analysis of the experiments including investigation and methodology. Visualization of results, writing and reviewing the manuscript. K.H., P.L., S.O., N.B., M.A., Y.L., Z.C., N.R., Q.T., J.X., F.S., D-C.H., S.W., A.J., H.N., K.Y.: Setting up individual models,

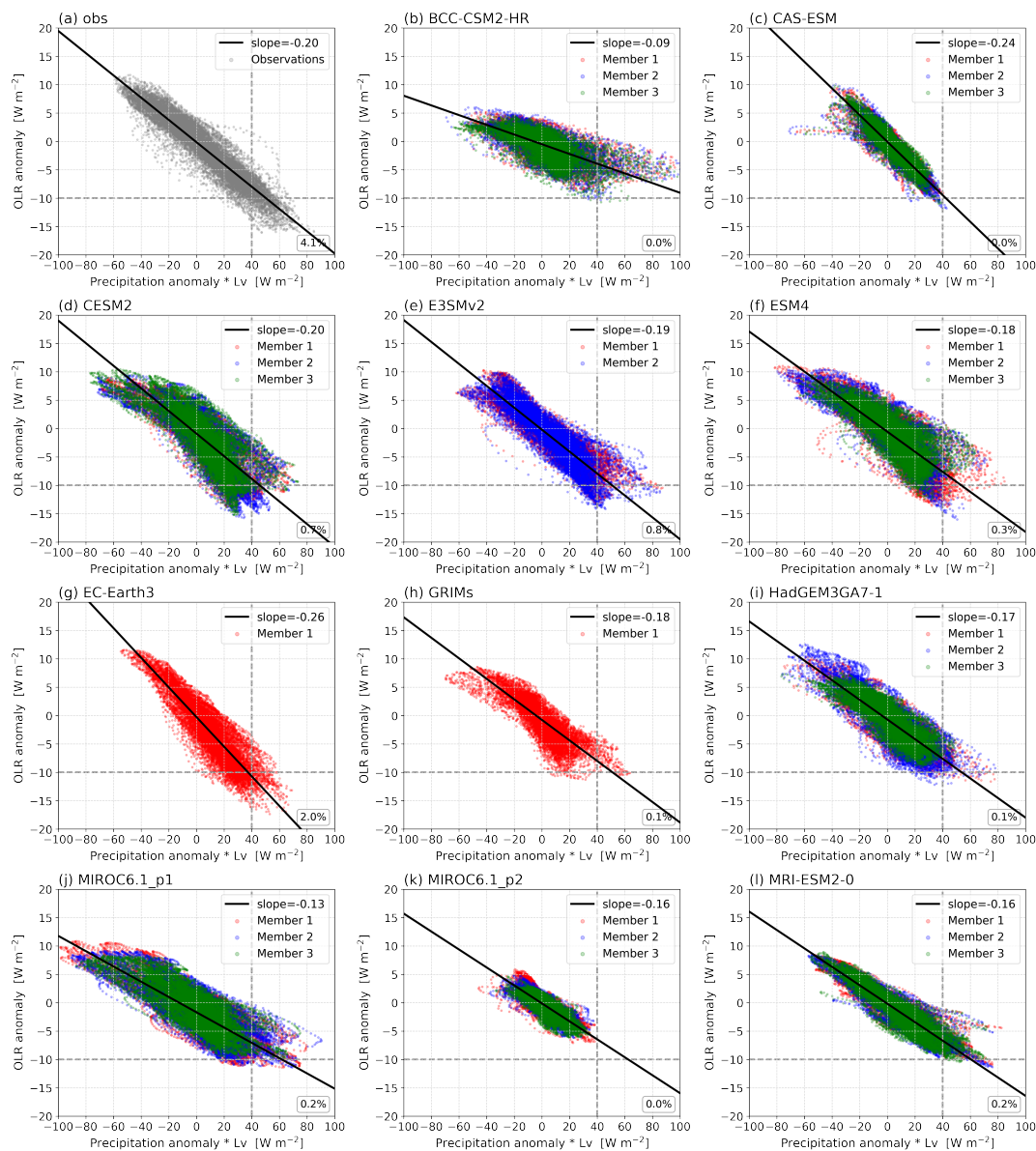


Figure 13. Scatter plots of the lead/lag regressed precipitation and OLR anomalies against RMM1 at each grid points over the Indo-Pacific region (15°S-5°N, 60°E-180°) from day -20 to day 20 in the boreal winter season (a) from observations using GPCP precipitation and NOAA OLR from 1997 to 2020, and (b)-(l) from QBOi phase 2 models from 1980 to 2020. The precipitation anomalies are timed by its latent heat releasing rate in the plots. Dots in red, blue, and green represents the results from member 1, 2, and 3 from the model, respectively. The linear regressed lines between two variables are denoted by the black lines with all ensemble members used. The linear regression coefficients are given by black numbers at the top right of each plot. The percentage of the sample dots with OLR anomalies below -10 W/m^2 and latent heating anomalies by precipitation above 40 W/m^2 is given by the number at the bottom right of each subplot.



running the experiments, and provision of data to the NERC CEDA archive. Reviewing the manuscript. N.B., J.A., Y.K., S.O., J.R.: Project management of QBOi, design of phase 2 experiments and data (diagnostic) request with input from the modelers.

335 *Competing interests.* JA serves as co-editor for the special issue to which this paper belongs. The remaining authors declare that they have no conflict of interest.

Acknowledgements. We acknowledge the scientific guidance of the World Climate Research Programme (WCRP) for helping motivate this work, coordinated under the framework of the Atmospheric Processes and their role in Climate (APARC, formerly Stratosphere-troposphere Processes and their Role in Climate) QBO initiative (QBOi). We acknowledge the Centre for Environmental Data Analysis (CEDA) for use of the Jasmin analysis platform and group workspace environment. K.H. and C-C.C. was supported by the U.S. Department of Energy, Office of Science, Office of Advanced Scientific Computing Research and Office of National Nuclear Security Administration, Scientific Discovery through Advanced Computing (SciDAC) program under Award Number O2307-089-049-010545, "Improving the quasi-biennial oscillation through surrogate-accelerated parameter optimization and vertical grid modification", funded through a National Science Foundation Inter Agency Agreement, Contract ID 1947282, and funding provided under Award Number 89233218CNA000001, funded through the Los Alamos National Laboratory, Subcontract number C5723. Part of this work was supported by the Regional and Global Model Analysis (RGMA) component of the Earth and Environmental System Modeling Program of the U.S. Department of Energy's Office of Biological & Environmental Research (BER) under Lawrence Livermore National Lab subaward DE-AC52-07NA27344, Lawrence Berkeley National Lab subaward DE-AC02-05CH11231, and Pacific Northwest National Lab subaward DE-AC05-76RL01830. K.H., Y.R., and N.R. were also supported by the National Science Foundation (NSF) National Center for Atmospheric Research, which is a major facility sponsored by NSF under Cooperative Agreement No. 1852977. C-H.P. was supported by the Basic Science Research Program through the National Research Foundation of Korea (NRF), funded by the Ministry of Education (RS-2025-25438815). S-W.S. and D-C.H. are supported by the National Research Foundation of Korea (NRF) grant funded by the Korea government (MSIT) (RS-2025-02363044). Y.K. was supported by the Japan Society for the Promotion of Science (JSPS KAKENHI; grant nos. JP26K00773, JP 25K01058, JP23K22574); the Environmental Restoration and Conservation Agency (Environment Research and Technology Development Fund; grant no. JPMEERF20242001); the Ministry of Education, Culture, Sports, Science, and Technology (MEXT; SENTAN program; grant nos. JPMXD0722680395). Z.C. was funded by the National Natural Science Foundation of China (42405170) and the Strategic Priority Research Program of Chinese Academy of Sciences (XDB0500303), and was technically supported by the National Large Scientific and Technological Infrastructure—Earth System Numerical Simulation Facility in China (<https://cstr.cn/31134.02.EL>). Part of this work was performed under the auspices of the U.S. Department of Energy (DOE) by Lawrence Livermore National Laboratory under contract DE-AC52-07NA27344. Q.T. and J.X. were supported as part of the Energy Exascale Earth System Model project, funded by the U.S. DOE, Office of Science, Office of Biological and Environmental Research. EC-Earth3 simulations were carried out thanks to an ECMWF Special project awarded to F.S.. S.W. was supported by JSPS KAKENHI Grant Number JP26K00773 and the MEXT Program for Advanced Studies of Climate Change Projection (SENTAN) Grant Number JPMXD0722681344. MIROC6.1 simulations were performed using the Earth Simulator at JAMSTEC. Y.L. was supported by the National Natural Science Foundation of China (42275056). H. N. and K. Y. were supported by the Japan Society for the Promotion of Science (JSPS KAKENHI; grant nos. 24K00710). K. Y. was supported by the Japan Society for the Promotion of Science (JSPS KAKENHI; grant nos. 24K00706).

340
345
350
355
360
365

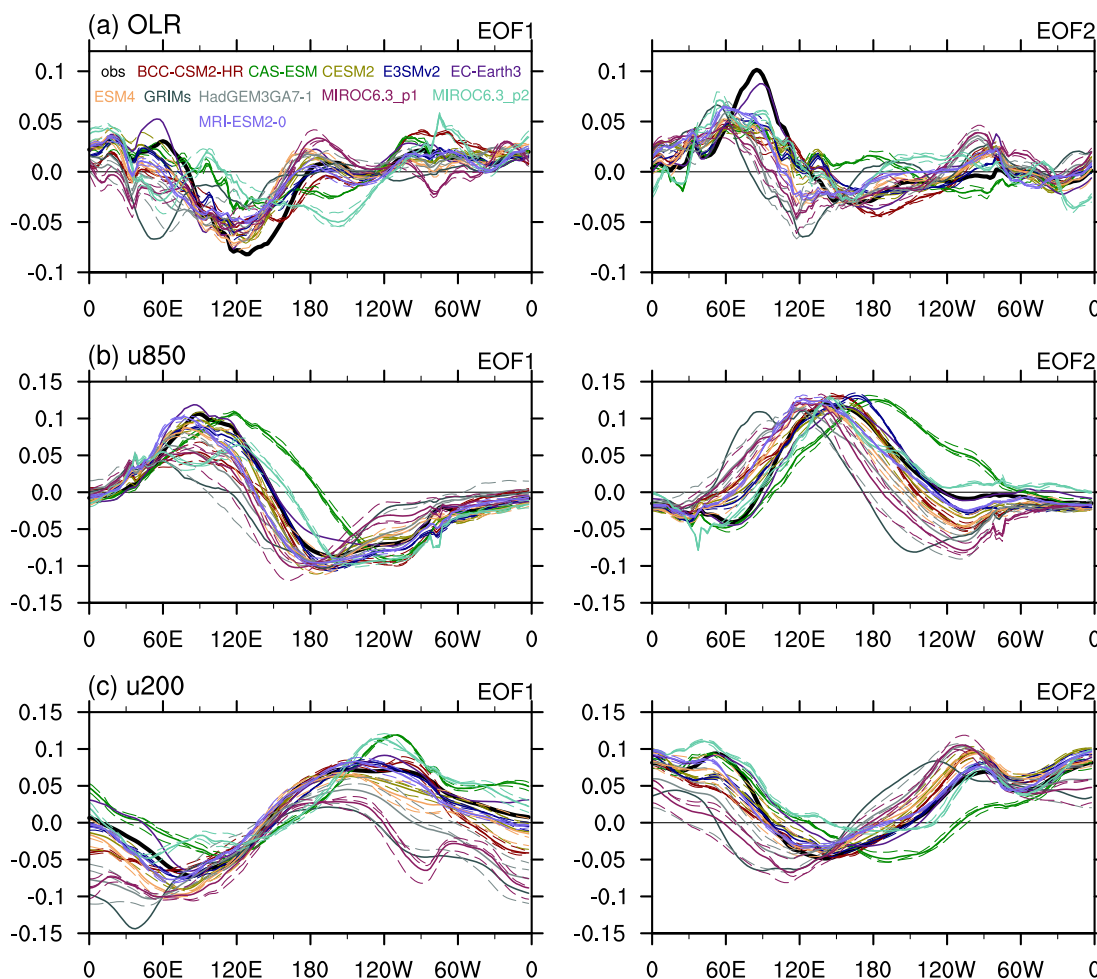


Figure A1. The two leading EOF patterns for the RMM indices derived from the observations and QBOi phase 2 models. Note that EOF1 and EOF2 are swapped for some models to guarantee the enhanced MJO convection is around the MC and WP longitudes in their patterns, respectively.

Appendix A: RMM index derivation for the QBOi phase 2 models

The RMM indices used in this study for the QBOi phase 2 models are derived from the outgoing longwave radiation (OLR), zonal wind at 200 hPa (u200), and zonal wind at 850 hPa (u850) in the model outputs. For each model, a combined Empirical Orthogonal Function (CEOF) analysis for these variables averaged around the equator is conducted to extract the two leading modes and the associated time series following Wheeler and Hendon (2004). The spatial patterns and their time series from the model CEOF analysis are swapped or adjusted for its sign to make sure the enhanced MJO convection in the two leading

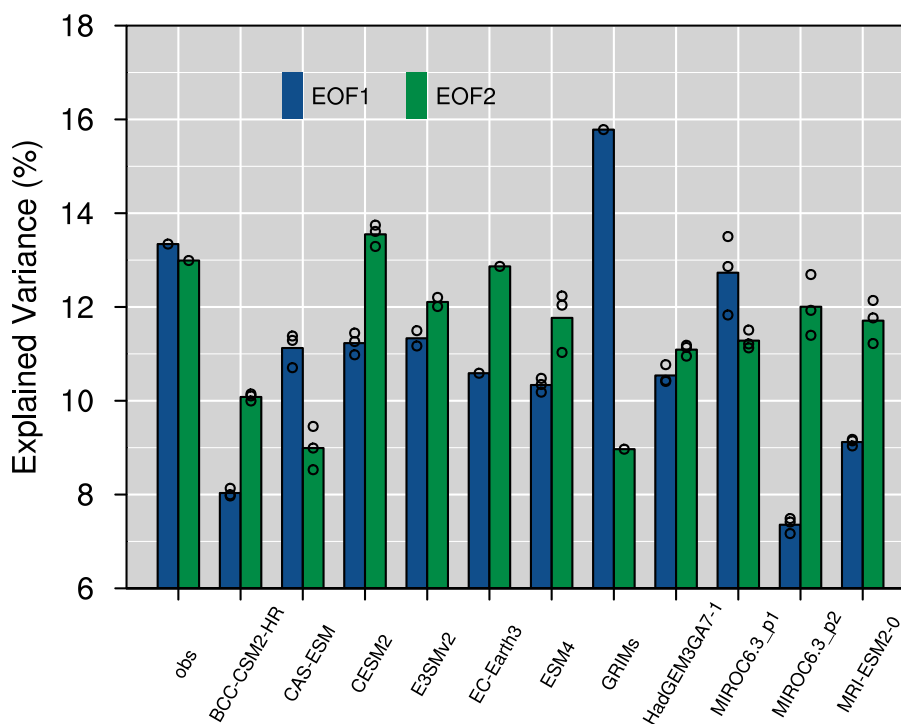


Figure A2. The explained variance of the two leading EOF patterns for the RMM indices derived from the observations and QBOi phase 2 models.

modes is at the same locations as in the observational results. The spatial patterns for the two leading EOF patterns are given by Fig.A1, and the fractions of their explained variance are shown in Fig.A2.



References

- 375 Adames, A. F. and Ming, Y.: Moisture and Moist Static Energy Budgets of South Asian Monsoon Low Pressure Systems in GFDL AM4.0, *Journal of the Atmospheric Sciences*, 75, 2107–2123, <https://doi.org/10.1175/jas-d-17-0309.1>, 2018.
- Adames, A. F. and Wallace, J. M.: Three-dimensional structure and evolution of the MJO and its relation to the mean flow, *Journal of the Atmospheric Sciences*, 71, 2007–2026, 2014.
- Andrews, M. B., Butchart, N., Anstey, J. A., Bednarz, E., Elsbury, D., García-Franco, J. L., Kumar, V., Palmeiro, F. M., Trencham, N. E.,
380 Yoshida, K., Chai, Z., Hong, D.-C., Huang, K., Jaison, A. M., Kawatani, Y., Knight, J. R., Lin, P., Lott, F., Lu, Y., Naoe, H., Osprey, S. M.,
Richter, J. H., Serva, F., Son, S.-W., Tang, Q., Watanabe, S., and Xie, J.: Extratropical teleconnections in a multi-model ensemble nudged
towards the observed QBO, *EGUsphere*, 2026, 1–33, <https://doi.org/10.5194/egusphere-2026-737>, 2026.
- Angulo-Umana, P., Kim, D., Blosssey, P. N., and Khairoutdinov, M.: Multiscale Convective Circulations and Scale Inter-
actions in a Global Storm-Resolving Model, *Journal of Advances in Modeling Earth Systems*, 18, e2025MS005 032,
385 <https://doi.org/https://doi.org/10.1029/2025MS005032>, e2025MS005032 2025MS005032, 2026.
- Anstey, J. A. and Shepherd, T. G.: High-latitude influence of the quasi-biennial oscillation, *Quarterly Journal of the Royal Meteorological
Society*, 140, 1–21, <https://doi.org/https://doi.org/10.1002/qj.2132>, 2014.
- Anstey, J. A., Butchart, N., Hamilton, K., and Osprey, S. M.: The SPARC Quasi-Biennial Oscillation initiative, *Quarterly Journal of the
Royal Meteorological Society*, 148, 1455–1458, <https://doi.org/https://doi.org/10.1002/qj.3820>, 2022.
- 390 Anstey, J. A., Butchart, N., Osprey, S., Kawatani, Y., Hamilton, K., Richter, J. H., Stockdale, T., Andrews, M. B., Chai, Z., Davini, P., Hong,
D.-C., Huang, K., Jaison, A. M., Kerzenmacher, T., Knight, J. R., Lin, P., Lott, F., Lu, Y., Naoe, H., Serva, F., Simpson, I., Son, S.-W.,
Tang, Q., Watanabe, S., Xie, J., and Yoshida, K.: Experiment design, nudging protocol, and models participating in Phase 2 of the APARC
Quasi-Biennial Oscillation initiative (QBOi), *EGUsphere*, 2026, 1–38, <https://doi.org/10.5194/egusphere-2026-1165>, 2026.
- Back, S.-Y., Han, J.-Y., and Son, S.-W.: Modeling Evidence of QBO-MJO Connection: A Case Study, *Geophysical Research Letters*, 47,
395 e2020GL089 480, <https://doi.org/https://doi.org/10.1029/2020GL089480>, e2020GL089480 2020GL089480, 2020.
- Baldwin, M. P., Gray, L. J., Dunkerton, T. J., Hamilton, K., Haynes, P. H., Randel, W. J., Holton, J. R., Alexander, M. J., Hirota, I., Horinouchi,
T., Jones, D. B. A., Kinnnersley, J. S., Marquardt, C., Sato, K., and Takahashi, M.: The quasi-biennial oscillation, *Reviews of Geophysics*,
39, 179–229, <https://doi.org/https://doi.org/10.1029/1999RG000073>, 2001.
- Butchart, N., Anstey, J. A., Hamilton, K., Osprey, S., McLandress, C., Bushell, A. C., Kawatani, Y., Kim, Y.-H., Lott, F., Scinocca, J.,
400 Stockdale, T. N., Andrews, M., Bellprat, O., Braesicke, P., Cagnazzo, C., Chen, C.-C., Chun, H.-Y., Dobrynin, M., Garcia, R. R., Garcia-
Serrano, J., Gray, L. J., Holt, L., Kerzenmacher, T., Naoe, H., Pohlmann, H., Richter, J. H., Scaife, A. A., Schenzinger, V., Serva, F., Versick,
S., Watanabe, S., Yoshida, K., and Yukimoto, S.: Overview of experiment design and comparison of models participating in phase 1 of the
SPARC Quasi-Biennial Oscillation initiative (QBOi), *Geoscientific Model Development*, 11, 1009–1032, <https://doi.org/10.5194/gmd-11-1009-2018>, 2018.
- 405 Collimore, C. C., Martin, D. W., Hitchman, M. H., Huesmann, A., and Waliser, D. E.: On The Relationship between the QBO and Tropical
Deep Convection, *Journal of Climate*, 16, 2552 – 2568, [https://doi.org/10.1175/1520-0442\(2003\)016<2552:OTRBTQ>2.0.CO;2](https://doi.org/10.1175/1520-0442(2003)016<2552:OTRBTQ>2.0.CO;2), 2003.
- Crook, J., Morris, F., Fitzpatrick, R. G. J., Peatman, S. C., Schwendike, J., Stein, T. H., Birch, C. E., Hardy, S., and Yang, G.-Y.: Impact of
the Madden-Julian oscillation and equatorial waves on tracked mesoscale convective systems over southeast Asia, *Quarterly Journal of
the Royal Meteorological Society*, 150, 1724–1751, <https://doi.org/https://doi.org/10.1002/qj.4667>, 2024.



- 410 EBDON, R. A. and VERYARD, R. G.: Fluctuations in Equatorial Stratospheric Winds, *Nature*, 189, 791–793, <https://doi.org/10.1038/189791a0>, 1961.
- Elsbury, D., Serva, F., Caron, J. M., Back, S.-Y., Orbe, C., Richter, J. H., Anstey, J. A., Butchart, N., Chen, C.-C., García-Serrano, J., Glanville, A., Kawatani, Y., Kerzenmacher, T., Lott, F., Naoe, H., Osprey, S., Palmeiro, F. M., Son, S.-W., Taguchi, M., Versick, S., Watanabe, S., and Yoshida, K.: QBOi El Niño Southern Oscillation experiments: assessing relationships between ENSO, MJO, and QBO, *Weather and*
- 415 *Climate Dynamics*, 7, 317–339, <https://doi.org/10.5194/wcd-7-317-2026>, 2026.
- Fu, X. H., Lee, J. Y., Wang, B., Wang, W. Q., and Vitart, F.: Intraseasonal Forecasting of the Asian Summer Monsoon in Four Operational and Research Models, *Journal of Climate*, 26, 4186–4203, <https://doi.org/10.1175/jcli-d-12-00252.1>, 2013.
- Hendon, H. H. and Abhik, S.: Differences in Vertical Structure of the Madden-Julian Oscillation Associated With the Quasi-Biennial Oscillation, *Geophysical Research Letters*, 45, 4419–4428, <https://doi.org/https://doi.org/10.1029/2018GL077207>, 2018.
- 420 Hersbach, H., Bell, B., Berrisford, P., Hirahara, S., Horányi, A., Muñoz-Sabater, J., Nicolas, J., Peubey, C., Radu, R., Schepers, D., Simmons, A., Soci, C., Abdalla, S., Abellan, X., Balsamo, G., Bechtold, P., Biavati, G., Bidlot, J., Bonavita, M., De Chiara, G., Dahlgren, P., Dee, D., Diamantakis, M., Dragani, R., Flemming, J., Forbes, R., Fuentes, M., Geer, A., Haimberger, L., Healy, S., Hogan, R. J., Hólm, E., Janisková, M., Keeley, S., Laloyaux, P., Lopez, P., Lupu, C., Radnoti, G., de Rosnay, P., Rozum, I., Vamborg, F., Villaume, S., and Thépaut, J.-N.: The ERA5 global reanalysis, *Quarterly Journal of the Royal Meteorological Society*, 146, 1999–2049,
- 425 <https://doi.org/https://doi.org/10.1002/qj.3803>, 2020.
- Hood, L. L. and Hoopes, C. A.: Arctic Sea Ice Loss, Long-Term Trends in Extratropical Wave Forcing, and the Observed Strengthening of the QBO-MJO Connection, *Journal of Geophysical Research: Atmospheres*, 128, e2023JD039501, <https://doi.org/https://doi.org/10.1029/2023JD039501>, e2023JD039501 2023JD039501, 2023.
- Houze Jr., R. A.: Mesoscale convective systems, *Reviews of Geophysics*, 42, <https://doi.org/https://doi.org/10.1029/2004RG000150>, 2004.
- 430 Huang, K., Richter, J. H., and Pegion, K. V.: Captured QBO-MJO Connection in a Subseasonal Prediction System, *Geophysical Research Letters*, 50, e2022GL102648, <https://doi.org/https://doi.org/10.1029/2022GL102648>, e2022GL102648 2022GL102648, 2023.
- Huang, K., Chen, C.-C., Moncrieff, M. W., and Richter, J. H.: A Multiscale Interaction Mechanism for the Observed QBO-MJO Connection, Under review at *Geophysical Research Letters*, <https://doi.org/10.22541/au.175924948.81063758/v1>, 2025a.
- Huang, K., Shields, C. A., Hall, K. R., Richter, J. H., Li, Y., and Chen, C.-C.-J.: Modulations of Atmospheric River Climatology by the Stratospheric Quasi-Biennial Oscillation, *Journal of Geophysical Research: Atmospheres*, 130, e2024JD042390,
- 435 <https://doi.org/https://doi.org/10.1029/2024JD042390>, e2024JD042390 2024JD042390, 2025b.
- Huffman, G. J., Adler, R. F., Morrissey, M. M., Bolvin, D. T., Curtis, S., Joyce, R., McGavock, B., and Susskind, J.: Global Precipitation at One-Degree Daily Resolution from Multisatellite Observations, *Journal of Hydrometeorology*, 2, 36 – 50, [https://doi.org/10.1175/1525-7541\(2001\)002<0036:GPAODD>2.0.CO;2](https://doi.org/10.1175/1525-7541(2001)002<0036:GPAODD>2.0.CO;2), 2001.
- 440 Jiang, X.: Key processes for the eastward propagation of the Madden-Julian Oscillation based on multimodel simulations, *Journal of Geophysical Research: Atmospheres*, 122, 755–770, <https://doi.org/https://doi.org/10.1002/2016JD025955>, 2017.
- Jiang, X., Adames, F., Kim, D., Maloney, E. D., Lin, H., Kim, H., Zhang, C., DeMott, C. A., and Klingaman, N. P.: Fifty Years of Research on the Madden-Julian Oscillation: Recent Progress, Challenges, and Perspectives, *Journal of Geophysical Research: Atmospheres*, 125, e2019JD030911, <https://doi.org/https://doi.org/10.1029/2019JD030911>, e2019JD030911 2019JD030911, 2020.
- 445 Kim, D., Sobel, A. H., Genio, A. D. D., Chen, Y., Camargo, S. J., Yao, M.-S., Kelley, M., and Nazarenko, L.: The Tropical Subseasonal Variability Simulated in the NASA GISS General Circulation Model, *Journal of Climate*, 25, 4641 – 4659, <https://doi.org/10.1175/JCLI-D-11-00447.1>, 2012.



- Kim, H., Caron, J. M., Richter, J. H., and Simpson, I. R.: The Lack of QBO-MJO Connection in CMIP6 Models, *Geophysical Research Letters*, 47, e2020GL087295, <https://doi.org/https://doi.org/10.1029/2020GL087295>, 2020.
- 450 Kim, H.-K. and Seo, K.-H.: Cluster analysis of tropical cyclone tracks over the western north pacific using a self-organizing map, *Journal of Climate*, 29, 3731–3751, 2016.
- Kim, H.-M., Zhou, Y., and Alexander, M. A.: Changes in atmospheric rivers and moisture transport over the Northeast Pacific and western North America in response to ENSO diversity, *Climate Dynamics*, 52, 7375–7388, <https://doi.org/10.1007/s00382-017-3598-9>, 2019.
- Lane, T. P.: Does Lower-Stratospheric Shear Influence the Mesoscale Organization of Convection?, *Geophysical Research Letters*, 48, e2020GL091025, <https://doi.org/https://doi.org/10.1029/2020GL091025>, e2020GL091025 2020GL091025, 2021.
- 455 Lee, H.-T.: NOAA Climate Data Record (CDR) of Daily Outgoing Longwave Radiation (OLR), Version 2.0., NOAA National Centers for Environmental Information., <https://doi.org/https://doi.org/10.25921/9pt5-by77.>, 2025.
- Lim, Y. and Son, S.-W.: QBO-MJO Connection in CMIP5 Models, *Journal of Geophysical Research: Atmospheres*, 125, e2019JD032157, <https://doi.org/https://doi.org/10.1029/2019JD032157>, 2020.
- 460 Lim, Y., Son, S.-W., Marshall, A. G., Hendon, H. H., and Seo, K.-H.: Influence of the QBO on MJO prediction skill in the subseasonal-to-seasonal prediction models, *Climate Dynamics*, 53, 1681–1695, <https://doi.org/10.1007/s00382-019-04719-y>, 2019.
- Liu, F. and Wang, B.: Impacts of upscale heat and momentum transfer by moist Kelvin waves on the Madden–Julian oscillation: a theoretical model study, *Clim Dynam*, 40, <https://doi.org/10.1007/s00382-011-1281-0>, 2013.
- Liu, F. and Wang, B.: Effects of moisture feedback in a frictional coupled Kelvin–Rossby wave model and implication in the Madden–Julian oscillation dynamics, *Clim Dynam*, 2016.
- 465 Liu, Y. and Tan, Z.-M.: Development of Shallow Convection and the Slow Eastward Propagation of Super Cloud Clusters in the Madden-Julian Oscillation, *Journal of Geophysical Research: Atmospheres*, 130, e2025JD043516, <https://doi.org/https://doi.org/10.1029/2025JD043516>, e2025JD043516 2025JD043516, 2025.
- Madden, R. A. and Julian, P. R.: Detection of a 40–50 day oscillation in the zonal wind in the tropical Pacific, *Journal of the atmospheric sciences*, 28, 702–708, 1971.
- 470 Madden, R. A. and Julian, P. R.: Description of global-scale circulation cells in the tropics with a 40–50 day period, *Journal of the atmospheric sciences*, 29, 1109–1123, 1972.
- Marshall, A. G., Hendon, H. H., Son, S.-W., and Lim, Y.: Impact of the quasi-biennial oscillation on predictability of the Madden–Julian oscillation, *Climate Dynamics*, 49, 1365–1377, 2017.
- 475 Martin, Z., Wang, S., Nie, J., and Sobel, A.: The Impact of the QBO on MJO Convection in Cloud-Resolving Simulations, *Journal of the Atmospheric Sciences*, 76, 669 – 688, <https://doi.org/10.1175/JAS-D-18-0179.1>, 2019.
- Martin, Z., Vitart, F., Wang, S., and Sobel, A.: The Impact of the Stratosphere on the MJO in a Forecast Model, *Journal of Geophysical Research: Atmospheres*, 125, e2019JD032106, <https://doi.org/https://doi.org/10.1029/2019JD032106>, e2019JD032106 2019JD032106, 2020.
- 480 Martin, Z., Orbe, C., Wang, S., and Sobel, A.: The MJO–QBO Relationship in a GCM with Stratospheric Nudging, *Journal of Climate*, 34, 4603 – 4624, <https://doi.org/10.1175/JCLI-D-20-0636.1>, 2021.
- Martin, Z. K., Simpson, I. R., Lin, P., Orbe, C., Tang, Q., Caron, J. M., Chen, C.-C., Kim, H., Leung, L. R., Richter, J. H., and Xie, S.: The Lack of a QBO-MJO Connection in Climate Models With a Nudged Stratosphere, *Journal of Geophysical Research: Atmospheres*, 128, e2023JD038722, <https://doi.org/https://doi.org/10.1029/2023JD038722>, e2023JD038722 2023JD038722, 2023.



- 485 Oh, J.-H., Kim, K.-Y., and Lim, G.-H.: Impact of MJO on the diurnal cycle of rainfall over the western Maritime Continent in the austral summer, *Climate dynamics*, 38, 1167–1180, 2012.
- Park, C.-H., Son, S.-W., Lim, Y., and Choi, J.: Quasi-biennial oscillation-related surface air temperature change over the western North Pacific in late winter, *International Journal of Climatology*, 42, 4351–4359, <https://doi.org/https://doi.org/10.1002/joc.7470>, 2022.
- Peatman, S. C., Matthews, A. J., and Stevens, D. P.: Propagation of the Madden–Julian Oscillation through the Maritime Continent
490 and scale interaction with the diurnal cycle of precipitation, *Quarterly Journal of the Royal Meteorological Society*, 140, 814–825, <https://doi.org/doi:10.1002/qj.2161>, 2014.
- Randall, D. A., Tziperman, E., Branson, M. D., Richter, J. H., and Kang, W.: The QBO–MJO Connection: A Possible Role for the SST and ENSO, *Journal of Climate*, 36, 6515 – 6531, <https://doi.org/10.1175/JCLI-D-23-0031.1>, 2023.
- Reed, R. J., Campbell, W. J., Rasmussen, L. A., and Rogers, D. G.: Evidence of a downward-propagating, annual wind reversal in the equa-
495 torial stratosphere, *Journal of Geophysical Research (1896-1977)*, 66, 813–818, <https://doi.org/https://doi.org/10.1029/JZ066i003p00813>, 1961.
- Sakaeda, N. and Torri, G.: The Behaviors of Intraseasonal Cloud Organization During DYNAMO/AMIE, *Journal of Geophysical Research: Atmospheres*, 127, e2021JD035749, <https://doi.org/https://doi.org/10.1029/2021JD035749>, e2021JD035749 2021JD035749, 2022.
- Sakaeda, N., Dias, J., and Kiladis, G. N.: The Unique Characteristics and Potential Mechanisms of the MJO–QBO Relationship, *Journal*
500 *of Geophysical Research: Atmospheres*, 125, e2020JD033196, <https://doi.org/https://doi.org/10.1029/2020JD033196>, e2020JD033196 10.1029/2020JD033196, 2020.
- Son, S.-W., Lim, Y., Yoo, C., Hendon, H. H., and Kim, J.: Stratospheric control of the Madden–Julian oscillation, *Journal of Climate*, 30, 1909–1922, 2017.
- Stan, C., Zheng, C., Chang, E. K.-M., Domeisen, D. I., Garfinkel, C. I., Jenney, A. M., Kim, H., Lim, Y.-K., Lin, H., Robertson, A., et al.:
505 Advances in the prediction of MJO teleconnections in the S2S forecast systems, *Bulletin of the American Meteorological Society*, 103, E1426–E1447, 2022.
- Toride, K. and Hakim, G. J.: Influence of Low-Frequency PNA Variability on MJO Teleconnections to North American Atmospheric River Activity, *Geophysical Research Letters*, 48, e2021GL094078, <https://doi.org/https://doi.org/10.1029/2021GL094078>, e2021GL094078 2021GL094078, 2021.
- 510 Tseng, K.-C., Maloney, E., and Barnes, E. A.: The Consistency of MJO Teleconnection Patterns on Interannual Time Scales, *Journal of Climate*, 33, 3471 – 3486, <https://doi.org/10.1175/JCLI-D-19-0510.1>, 2020.
- Vincent, D. G.: The South Pacific Convergence Zone (SPCZ): A Review, *Monthly Weather Review*, 122, 1949 – 1970, [https://doi.org/10.1175/1520-0493\(1994\)122<1949:TSPCZA>2.0.CO;2](https://doi.org/10.1175/1520-0493(1994)122<1949:TSPCZA>2.0.CO;2), 1994.
- Waliser, D. E. and Gautier, C.: A Satellite-derived Climatology of the ITCZ, *Journal of Climate*, 6, 2162 – 2174, [https://doi.org/10.1175/1520-0442\(1993\)006<2162:ASDCOT>2.0.CO;2](https://doi.org/10.1175/1520-0442(1993)006<2162:ASDCOT>2.0.CO;2), 1993.
515
- Wang, B., Chen, G., and Liu, F.: Diversity of the Madden-Julian Oscillation, *Science Advances*, 5, <https://doi.org/10.1126/sciadv.aax0220>, 2019.
- Wang, J., Kim, H.-M., and Chang, E. K. M.: Interannual Modulation of Northern Hemisphere Winter Storm Tracks by the QBO, *Geophysical Research Letters*, 45, 2786–2794, <https://doi.org/https://doi.org/10.1002/2017GL076929>, 2018a.
- 520 Wang, J., Kim, H.-M., Chang, E. K. M., and Son, S.-W.: Modulation of the MJO and North Pacific Storm Track Relationship by the QBO, *Journal of Geophysical Research: Atmospheres*, 123, 3976–3992, <https://doi.org/https://doi.org/10.1029/2017JD027977>, 2018b.



- Wheeler, M. and Kiladis, G. N.: Convectively coupled equatorial waves: Analysis of clouds and temperature in the wavenumber-frequency domain, *Journal of the Atmospheric Sciences*, 56, 374–399, [https://doi.org/10.1175/1520-0469\(1999\)056<0374:ccewao>2.0.co;2](https://doi.org/10.1175/1520-0469(1999)056<0374:ccewao>2.0.co;2), 1999.
- 525 Wheeler, M. C. and Hendon, H. H.: An all-season real-time multivariate MJO index: Development of an index for monitoring and prediction, *Monthly Weather Review*, 132, 1917–1932, [https://doi.org/10.1175/1520-0493\(2004\)132<1917:aarmmi>2.0.co;2](https://doi.org/10.1175/1520-0493(2004)132<1917:aarmmi>2.0.co;2), 2004.
- Yoo, C. and Son, S.: Modulation of the boreal wintertime Madden-Julian oscillation by the stratospheric quasi-biennial oscillation, *Geophysical Research Letters*, 43, 1392–1398, 2016.
- Zhang, C. D.: Madden-Julian oscillation, *Reviews of Geophysics*, 43, 36, <https://doi.org/10.1029/2004rg000158>, 2005.